5-9-2015

Spectroscopic Studies of Cyanine Dyes and Serum Albumins for Bioanalytical Applications

Erica Lewis
elewis23@gsu.edu

SPECTROSCOPIC STUDIES OF CYANINE DYES AND SERUM ALBUMINS FOR BIOANALYTICAL APPLICATIONS

by

ERICA VANESSA LEWIS

Under the Direction of Gabor Patonay, PhD

ABSTRACT

The use of cyanine dyes in bioanalytical applications has become a widely explored topic of interest in chemistry. Their ability to absorb and fluoresce in the UV-visible and near-infrared region of the electromagnetic spectrum benefits their use as imaging probes and fluorescent labels due to the reduced auto-fluorescence from biological molecules. The behavior of these dyes lies in their structure which consists of two nitrogen containing heterocycles joined by an electron deficient polymethine bridge that allows specific energy transitions to occur. The first portion of this work aims to explore dye functionality for analytical applications regarding the non-covalent labeling of bovine serum albumin. The second portion of the work explores dye interactions with human serum albumin in biological membrane mimetic environments using the ternary system of sodium dioctyl sulfosuccinate (AOT) in water and *n*-heptane.

INDEX WORDS: Cyanine, Dyes, Analytical, Non-covalent, Labels, Albumins, Reverse micelles

SPECTROSCOPIC STUDIES OF CYANINE DYES AND SERUM ALBUMINS FOR BIOANALYTICAL APPLICATIONS

by

ERICA VANESSA LEWIS

A Thesis Submitted in Partial Fulfillment of the Requirements for the Degree of

Master of Science

in the College of Arts and Sciences

Georgia State University

2015

SPECTROSCOPIC STUDIES OF CYANINE DYES AND SERUM ALBUMINS FOR BIOANALYTICAL APPLICATIONS

by

ERICA VANESSA LEWIS

Committee Chair: Gabor Patonay

Committee: Maged Henary

Gangli Wang

Electronic Version Approved:

Office of Graduate Studies

College of Arts and Sciences

Georgia State University

May 2015

DEDICATION

I would like to dedicate this work first and foremost to my mother, Patti Ann Lewis. You are everything to me and I'm happy to have had you in my life for those moments in time. I can't imagine what my life would have been like if I had never met you. I really just wanted to take the time to thank you for instilling in me all of what you could while you were here. During the bad times, you were still strong, and fought the hardest of battles. You're brightest star in my sky and you will forever shine above me. I want to thank you for loving me so unconditionally from the bottom of your heart because I still feel your love every day. You are the very best of me, and for that I cannot thank you enough. I love you.

I'd also like to dedicate this work to my father, Eric Van Lewis: You probably don't realize this, but I think you knew more than you believed you did. My life would be nothing without you and it's because of you that my journey was possible. I love you.

To all of my family members near and afar: each one of you has had a hand in shaping my life and character. I love you all so much and I thank you all for everything that you've done.

ACKNOWLEDGEMENTS

I would like to begin by acknowledging my primary investigator, Dr. Gabor Patonay: Never will I forget the advice and independence that you have given me over the years. I am going to cherish all that I have learned from your guidance, throughout my career as a chemist. To my additional committee members, Dr. Maged Henary and Dr. Gangli Wang, I truly want to give you my thanks for challenging me during my defense and allowing me to share my work. You have all helped shape my skills a chemist and I am very hopeful for the future. You've built up my confidence and I am so very thankful. To Dr. Garfield Beckford and Gala Chapman: Never could I have made it this far without the two of you and your support. Thank you for going above and beyond to help and guide me; not just as my mentors, but as friends too. I hope to use all of what I have learned from you two because you have both given me the motivation to let myself seek bigger and better things. Next I would like to mention Dr. Yogesh Yadav: thank you for generously providing me with the functional dyes for my project. I see many good things down the road for you and I wish you the very best. To Andrew Levitz: thank you so much for never getting mad at me when I asked for more of your dyes for my project; I appreciate you going out of your way to help me because I could not have done it otherwise. It was all worth it! To Cory Holder, Vincent Martinez, Eduardo Soriano, Deirdre Stinnett, and Tyler Dost: I tried to run from organic chemistry, but you were all a part of helping me strengthen my skills in and around the lab, and helped me prove to myself that I would not be defeated by it. Thank you all and I wish you the best in your future careers. To the Patonay Group in Kell 594: From the vast desert of the 4.5th floor, to the murky waters of our flooded lab, and the sweet smell of asbestos, you and only you guys will be able to look back with joy at all of the moments we have shared.

I want to thank each and every one of you, Eman Alsolmy, Walid Abdelwahab, Jennifer Novak, Edjohnier Phillips, Kyle Emer, Andrew Puetz, and Katie Kiernan. It was all of you who made me laugh on my worst days and laugh even harder on my good days. I enjoyed every moment working and researching with you guys. I am going to miss you all so very much and I truly do wish all of you the best of luck and success in your careers. You're all so talented in so many ways and I know that you're all more than capable of carrying on the legacy of our research group.

TABLE OF CONTENTS

LIST OF TABLES

LIST OF FIGURES

1 INTRODUCTION

The whole of synthetic dyes encompasses a vast range of behavior, classification, and function. Known for their striking colors and photosensitizing properties, cyanine dyes have gained a great deal of interest for their applications in bioanalytical chemistry. The origin of these applications began with the discovery of Cyanine Blue by C.H. Greville Williams.[1]

The commercial textile dyeing industry saw its first major success in 1856 when W.H. Perkin synthesized Mauve, a steadfast dye that colored fabrics a brilliant purple.[1] In the same year, C.H.G. Williams synthesized Cyanine Blue, which gave off a brilliant blue color in solution, but held poorly to the fibers of the fabrics and decomposed with prolonged exposure to light.[1-2] This unusual light sensitization went largely unnoticed until 1873, nearly 20 years after its discovery, when H.W. Vogel found that adding Cyanine Blue to a silver bromide based photographic film enhanced its spectral sensitivity.[1-3] The light absorbed by the film was extended to the ultraviolet-visible (UV-vis) and to the near infrared (NIR) regions of the electromagnetic spectrum.

Upon the discovery of its newfound application, Cyanine Blue was considered to be the most powerful photosensitizer of the time, which opened the door to a new world of cyanine dyes. Taking these light sensitive properties into account, it is not uncommon to find cyanines used in diode lasers, optical recording media, electronic devices, solar cells, and a host of other applications.[4-6]

1.1 Aim of work

Given the versatility in utilization of cyanine dyes and their unique spectral properties, it is the goal of this work to examine the suitability of two classes of polymethine cyanine dyes for their use in bioanalytical applications via absorbance and fluorescence spectroscopies.

General spectroscopic binding studies of cyanine dyes and proteins can be readily found in scientific literature. These studies are typically conducted in bulk solvents with the verification of binding interactions observed spectroscopically. The goal of the first portion of this work is to examine the spectral behavior of three trimethine cyanine dyes and their interactions with bovine serum albumin. This study is meant to serve as a general model study of dye characterization and dye-protein interactions. The methods applied in these experiments are ones typically employed in bioanalytical studies which are widely accepted as valid models for dye-protein binding interactions.

However, fewer studies have examined the nature of cyanine dye interactions with proteins in restricted areas rather than in bulk solutions. Given the differences between continuous solvent systems and more confined settings such as those observed *in vivo*, it is of interest to study dye-protein interactions under these contrasting conditions. Thus, the second portion of this work aims to explore the potential analytical utility of examining the effects of confinement on the binding interactions between two novel heptamethine cyanine dyes and human serum albumin using reverse micelles as a confined biomembrane mimetic system.

1.2 Quantum mechanics of cyanine dye behavior

The experiments described in this work are based on the spectroscopic analyses of each dye's absorptive and emissive behaviors. Accordingly, such studies require the

acknowledgement of the quantum mechanical considerations that describe their unique spectral behavior.

1.2.1 Early discoveries in quantum mechanics

The basis of cyanine dye behavior stemmed from the realization of the quantization of energy – a drastic departure from using classical mechanics to explain molecular behavior. This shift in thought began with new descriptions for unexplained phenomena such as blackbody radiation and the emission spectrum of hydrogen.[11] Max Planck theorized that deviations in microscopic behavior from that of classical explanations were the results of discrete values of energy. Though not widely accepted, his concept was based on empirical data that could be described by the equation:

$$E = nhv \qquad (1)$$

where n is a positive integer, h was an unknown constant of proportionality, and v was the frequency of the light wave.[7]

A more refined explanation was given by Albert Einstein who verified the quantization of energy with his experiments relating to the photoelectric effect.[7] The results of these experiments determined that energy radiated from a beam of light could be concentrated in a single electron, thus defining the term, photon, which is essentially a packet of localized light behaving as a particle.[7-8] This behavior could then be described by the equation:

$$E = hv \qquad (2)$$

Where h was verifiably determined to be 6.626×10^{-34} J·s, termed Planck ’s constant, and v was the frequency at which the energy is quantized. Louis de Broglie maintained that this

behavior should also be associated with the wavelength and the momentum (p) of a light particle through his equation:

$$\lambda = \frac{h}{p} \qquad (3)$$

This equation suggested that light could behave as both a particle and a wave. This controversial theory was confirmed by the experiments of Davisson and Germer, which gave rise to the notion of wave-particle duality.[7] The accumulation of these discoveries contributed to the characterization of microscopic systems, which could ultimately be used to elucidate spectral behavior on a molecular level.

1.2.2 The absorption and emission of light

Einstein's experiments showed that the electrons in a system could absorb energy from a beam of light at a certain frequency, which was consequently of a specific energy.[11] Thus, an electron of an initial energy can be promoted to a state of higher energy when it absorbs a photon through a process called excitation – as given by the equation[7-9]:

$$h\nu = |E_2 - E_1| \qquad (4)$$

where E_1 is the initial energy of the electron and E_2 is the energy of the electron after it has been excited. The various electronic transitions of the system can be visualized easily by Jablonski's Diagram as shown in Figure 1.1, where S_n denotes the specific energy level: S_0 is the ground state, and levels thereafter are various excited states.[8]

After the electron is excited, collisions and vibrational movements cause the absorbed energy to be released from the electron through a process called internal conversion (IC). The

accrued energy can be lost as heat, or by the emission of a photon of lower energy, called fluorescence.[8]

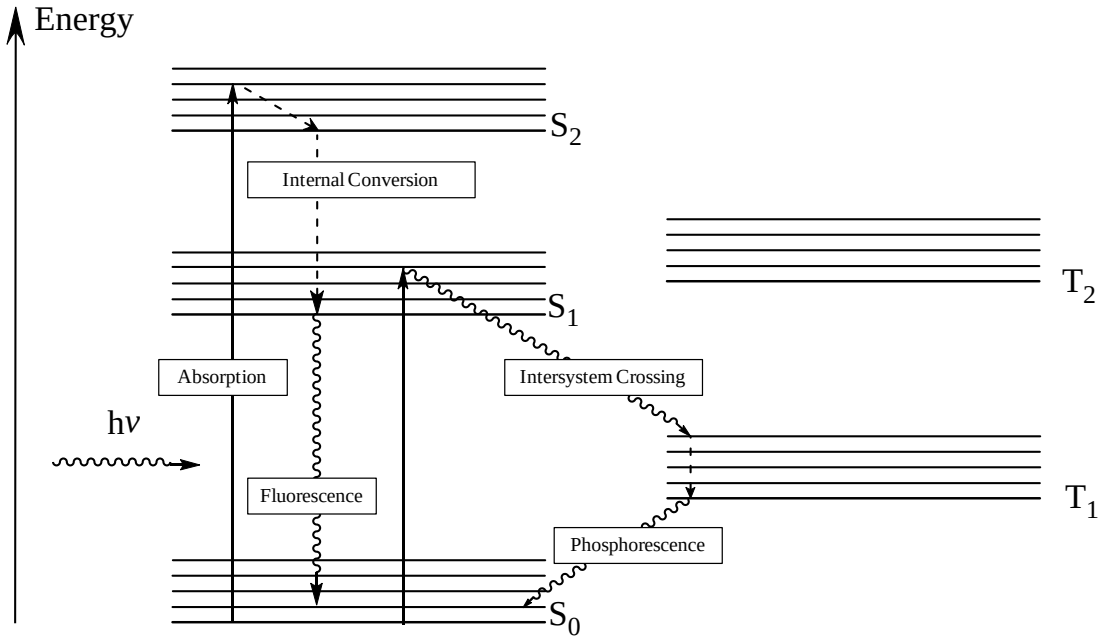

Figure 1.1 Jablonksi's Diagram

Alternatively, rather than falling back down to the ground state, the electron can undergo what is called, intersystem crossing (ISC), wherein the spin of the electron changes, and it is thus promoted it to an excited triplet state, T_n. From there, the electron can fall back down to its ground state S_0 and emit light in a process known as phosphorescence. [8]

These principles can be exhibited by cyanine dyes, particularly those of the polymethine class; where of these dyes, several subclasses such as azocarbocyanines, hemicyanines, and diazahemicyanines can be derived.[13] An examination of the general polymethine dye structure gives insight into their absorptive and emissive behaviors.

1.2.3 Structural contributions to cyanine dye behavior

The general structure of a cyanine dye (Figure 1.2) consists of two nitrogen containing ring systems joined by an electron deficient methine bridge, where *n* indicates the number of methine components.[1-3, 10] This electron deficient bridge ultimately results in a non-bonding highest occupied molecular orbital (HOMO), which narrows the energy gap between it and the lowest unoccupied molecular orbital (LUMO).[14] When compared to a dye with an electron sufficient linker of a similar chain length, the larger energy gap between the HOMO and LUMO of this compound would be a much wider, thus resulting in a higher energy absorption band.[11]

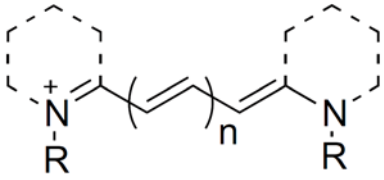

Figure 1.2 General structure of a polymethine cyanine dye

The nitrogen atoms are tri- and tetravalent respectively, and the methine chain can reside at the *ortho* and/or *para* position of the two atoms.[10] Furthermore, the chain can be extended to contain an increased odd number of carbon atoms, which in turn, indicates the name of the compound: werein *n* = 0, 1, 2, and 3 are monomethine, trimethine, pentamethine, and heptamethine respectively. The aromatic ring systems can be derived from various heterocycles as shown in Figure 1.3, including, but not limited to: quinoline, benzoquinoline, benzimidazole, pyridine, benzothiazole, benzoxazole, indole, benzindole, and many more.[10]

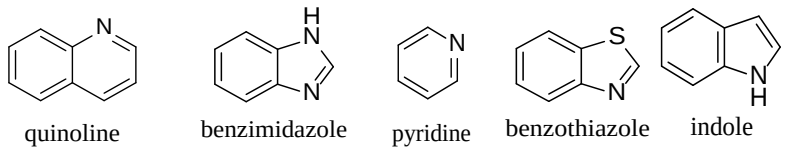

Figure 1.3 Typical heterocycles incorporated into cyanine dye structures

Referring back to Figure 1.2, the typical structure of a polymethine cyanine dye contains two nitrogen containing heterocycles joined by an apparent conjugated system of alternating pi and sigma bonds. However, it is more precise to think of this linker as a resonant bridge wherein the electrons are delocalized equally over the whole of the polymethine chain.[9] This behavior is similar to that of the C–C bonds in benzene, which further confers its stability.[9] Moreover, the conjugated system of the linker allows for many resonance structures to be formed, but the most important ones are those that leave the lowest electron density on the nitrogen atoms.[10] The electrons contained within this system are attracted to the positively charged nitrogen on either heterocycle.[7, 9] Upon excitation of these electrons with an appropriate amount of energy, the notable characteristics of these dyes can be observed.

An expansion of (4) relates wavelength to transitions between energy levels:

$$\lambda = hc/\Delta E \qquad (5)$$

where again h is Planck's constant, c is the speed of light, and ΔE is the difference in energy between the excited energy state and the perceived normal or ground state of the electron.[7, 9] From this equation, it is possible to predict the wavelength of maximum absorbance, wherein the transition energy of an electron from its ground state to excited state is the greatest. While the equations explained above describe the electronic behavior of single dye molecules, it is of equal importance to describe the collective behavior of dye molecules that can be encountered during a typical analysis.

1.2.4 The aggregation behavior of cyanine dyes

One of the most common behaviors of cyanine dyes is their ability to self-associate into different supermolecular structures called aggregates. Aside from existing in its monomeric form, where the dye is free to move, aggregates include H- and J-type aggregation. The aggregation behaviors observed in cyanine dyes have been well-studied phenomena due to their intermediate position between dissolved molecules and ordered crystals.[11] Beckford and coworkers mention that small angular slippages ($\alpha > \sim 32$) among these molecules result in H-aggregation, and large angular molecular slippage ($\alpha < \sim 32°$) results in J-aggregation. J-aggregation is similar to that of a "brickwork" arrangement H-aggregates assume a "card pack" arrangement".[12] Guralchuk and coworkers point out that in some cases, H-aggregates, and J-aggregates can both appear on an absorption spectrum, which corresponds to the "herringbone" arrangement of the dye molecules.[13] Kim and coworkers point out that J-aggregates are generally more fluorescent than H-aggregates, but are quenched in the presence of biomolecules.

1.2.5 Dye aggregate formation

Dipole–dipole interactions between passing dye monomers making up the aggregates induce the transfer of electronic excitation throughout the entirety of the aggregate. This highly ordered system them produces a coherent delocalized excitation.[14] This excitation or, exiciton is the result of the collective oscillation of adjacent dipoles in an a dye aggregate. This association leads to an enhancement of the transition oscillator strength, thus increasing the chance of absorption and emission.[14] Furthermore, in the context of this theory, the molecule is considered to be a point dipole and the excitonic state of the aggregate is split into two levels: an upper and a lower state.[10] From there, the dye molecules can aggregate in a parallel formation (plane-to-plane), resulting from parallel transitions in the upper state to form the H-aggregate formation, or

a head-to-tail formation resulting from perpendicular transition moments to a lower state, in the form of a J-aggregate.[15] Additionally, the structure of the dye, the polarity of the solvent, pH, ionic strength, and temperature can all have a strong effect on the type of aggregation observed[12, 16].

1.3 The utilization of cyanines in bioanalytical chemistry

The shortcomings of Cyanine Blue for use as a traditional dye demonstrated a key property of synthetic dyes: chemical functionality. As Matsuoka points out, in the historic sense, the development of traditional dyes focused on their use as coloring agents for textiles and plastics, whereas functional dye synthesis focuses heavily on efficient light absorption.[10] Advances in bioanalyses have made use of these dyes as fluorescent labels,[17] chemical sensors,[18]and pH probes.[17-19] Additionally, analytical techniques such as high performance liquid chromatography (HPLC) and capillary electrophoresis (CE) have employed the use of cyanine dyes for the ultra-trace detection of proteins through both covalent and non-covalent interactions.[20] Moreover, absorbance and fluorescence spectroscopies are powerful tools for examining cyanine dye behavior as well as its interactions with various biological molecules.

1.3.1 Spectroscopic analysis

Given the absorptive and emissive properties that cyanines possess, the use of spectroscopic means to monitor these electronics has proven to be an invaluable tool in bioanalytical methods.

1.3.1.1 Absorbance spectroscopy

The utilization of absorbance spectroscopy relies on the interactions between sample molecules and photons. Spectrophotometers are designed to measure the amount of light that a

sample absorbs and does not absorb.[8] A basic spectrophotometer is equipped with four simple components: a light source, a wavelength selector, a sample compartment, and a detector. The measurement function of this instrument relies on the principle of transmittance, T, or the fraction of original light passing through the sample as given by equation 6:

$$T = \frac{I}{I_0} \qquad (6)$$

Where I_0 is the original amount of light that passes through the sample and I is the amount of light that emerges from the other side of the sample. Generally, the transmittance is expressed as *percent transmittance* (%T) by multiplying the resultant T by 100.[8] The value of the transmittance can be used to calculate the absorbance of a species as shown in equation 7:

$$A = -\log T \qquad (7)$$

The value of absorbance, A, is directly proportional to the concentration of the absorbing species as given by the Beer-Lambert Law:

$$A = \varepsilon bc \qquad (8)$$

where b is the pathlength of the sample cell, c is the concentration of the sample, and ε is the molar absorptivity of the species. The quantity ε is a constant of proportionality that essentially describes how much light a species absorbs at a particular wavelength, which is an important parameter in dye characterization because it is attributed to is absorbing efficiency.[8] It

is this relationship that serves as the basis for spectrophotometry and is upon which the following experiments will rely.[8]

1.3.1.2 Fluorescence spectroscopy

In addition to absorbance spectroscopy, the processes after absorption are of particular interest in bioanalytical applications. Fluorescence detection is also a common use of cyanine dyes which makes their emissive behavior a crucial element of study. As mentioned previously, excited molecules undergo several processes of relaxation and energy loss as they fall back down to their ground state. As the molecule returns to its ground state, its remaining energy can be released as a photon, which can be measured with fluorescence spectroscopy.[8] A spectrofluorometer or fluorometer consists of the same components as a spectrometer, with the addition of a second wavelength selector and a second detector. In this case, the second detector and wavelength selector are positioned perpendicular to the sample compartment for the detection of emission. Therefore, cuvettes must be designed to accommodate transmited light from this direction.[8] Fluorescence detection can be used to observe monomeric and aggregated dye behaviors as well as binding interactions between a dye and the species of interest.

1.3.1.3 Spectral detection of cyanine dyes

The way in which the dyes aggregate can provide more information about spectral results that may be obtained in analysis. In the case of H-aggregation, the absorption maxmium shifts hypsochromically with respect to the monomer band. J-aggregates are characterized by a narrow absorption band that is red shifted in comparison to the monomer band. The resulting redshift of the J-aggregate is caused by the delocalization of the excited electrons over the aggregated dye molecules through intermolecular reactions between two transition dipole moments.[21]

1.4 Final remarks regarding cyanine dye behavior

The versatility of analytical chemistry allows it to be used in all facets of chemistry. Thus, these principles can be applied in applications involving biological components such as proteins. As more discoveries in the area of bioanalytical chemistry are made, it is of great importance to develop novel techniques and methods to ensure the most precise and accurate results. Therefore, the goal of the following projects aims to demonstrate the bioanalytical utility of examining variances in cyanine dye-protein binding interactions in bulk solvents and confined biomembrane mimetic environments. In this regard, the problems to be addressed are the nature of their interactions as well as the extent of their interactions. By using the processes described above, both qualitative and quantitative information is being sought through chemcial analyses.

2 A BINDING STUDY OF TRIMETHINE DYES AND BOVINE SERUM ALBUMIN

2.1 Serum albumin analysis with cyanine dyes

Many analytical methods exist for studying the binding sites of proteins as well as their interactions with various ligands. These methods include displacement by ultrafiltration or equilibrium dialysis, crystallographic studies of complexes with proteins, site directed mutagenesis, affinity capillary electrophoresis, and competitive zonal elution through high performance liquid chromatography (HPLC).[22] Additionally, the use of a non-functionalized dye with an affinity for the protein in question is beneficial for such bioanalytical studies.[20] For example, the aggregation behavior of certain cyanines has been utilized for the detection of proteins due to their brilliant color changes.[17] Thus as more dyes are being developed for such applications, it is of importance to obtain information regarding their intrinsic absorptive and emissive behaviors as well as the extent of their affinity for the target protein.

2.1.1 Bovine serum albumin

The manufacturing process for various viral vaccines utilizes fetal bovine serum (FBS) during production. Bovine serum albumin (BSA) is a major transport protein of fetal bovine serum (FBS) and as Loughney and coworkers point out is a known allergen.[23] Specifically, certain individuals with allergies to milk, beef, or cow dander are at a higher risk for developing respiratory problems as well as rhinoconjunctivitis.[24] Thus, methods of analysis are necessary for the detection of this protein. Therefore, it is of interest to utilize the spectroscopic properties of cyanine dyes for the detection of BSA.

BSA is a globular protein made up of three major domains that each contain two subdomains: IIA and IIIA.[25] The subdomains are stabilized by 17 disulfide bridges that help to form their specific binding pockets. Both subdomains contain intrinsic fluorescent residues Trp 214 and Tyr 411 in IIA and IIIA respectively. Trp 214 displays the most fluorescence in the molecule, Tyr displays moderate fluorescence, but is quenched in the presence of amino groups, carboxyl groups, or tryptophan residues.[26] These hydrophobic residues are the binding sites of interest for non-covalent interactions with cyanine dyes. Furthermore, as Pisoni and coworkers point out, steric interferences can also affect dye and protein binding interactions.[25]

2.1.2 Spectroscopic determination of cyanine dye and protein binding affinities

Association constants between various species can be determined through spectroscopic measurements.[8] As mentioned previously, the absorbance and fluorescence spectra of a dye can be altered based on variations in its microenvironment. By adding incremental amounts of albumin to a series of solutions containing a constant concentration of dye, the spectral changes of the dye can be observed and related to the amounts of albumin added. The binding constant between two species can be determined according to the following equilibrium expressions:

$$D + P \leftrightarrow DP \qquad (10)$$

$$K = \frac{[DP]}{[D]_f[P]_f} \qquad (11)$$

By introducing the equation for mass balance, the equilibrium expression of the system can be described according to the following:

$$[D]_T = [DP] + [D]_f \qquad (12)$$

$$\frac{[DP]}{[P]} = K_s[D]_f = K_s([D]_T - [DP]) \qquad (13)$$

$$\frac{[DP]}{[P]} = -K[DP] + K_s[D]_T \qquad (14)$$

Therefore, a plot of [DP]/[P] as a function of [DP] should yield a straight line with a slope of negative K that describes the concentrations of dye-protein interactions with respect to the free species in solution.[8] These values can be determined by spectroscopic measurements.

Expanding on Beer's Law, it is apparent that absorbance is additive and thus the absorbance of a solution at any wavelength is the sum of the absorbances of all of the species in the solution and is thus:[8]

$$A = \Sigma \varepsilon b[n] \qquad (15)$$

where ε is the molar absorptivity of each of the species at a particular wavelength, b is the pathlength, and [n] is the concentration of each species in the mixture. Thus, obtaining molar absorptivity values for the various species in solution can help deconstruct any spectral results obtained experimentally.

According to Beckford and coworkers, the Scatchard Method can also be utilized with fluorescence measurements.[12] The same equilibrium expression as shown in (11) can be used in conjunction with variations in fluorescence intensities to determine the concentrations of the interacting species at equilibrium:

$$\frac{1}{\Delta F} = \frac{1}{k[D]} + \left(\frac{1}{k[D]K}\right)\frac{1}{[P]} \quad (16)$$

where ΔF is the change in the fluorescence intensity of the dye-protein complex and *k* is a constant relating to emissive processes. The equilibrium constant can be determined by creating a double reciprocal plot of the change in fluorescence intensity as a function of the concentration of the protein. As described by the equation, dividing the intercept by the slope should yield the binding constant, K.

2.1.3 Purpose of study

This study aims to characterize a series of novel trimethine dyes (Figure 2.1) and examine their binding behavior with bovine serum albumin. Specifically, the effects of side chain length and heterocyclic substitution were taken into consideration when evaluating their intrinsic absorptive and emissive properties and the changes in these properties upon interaction with bovine serum albumin.

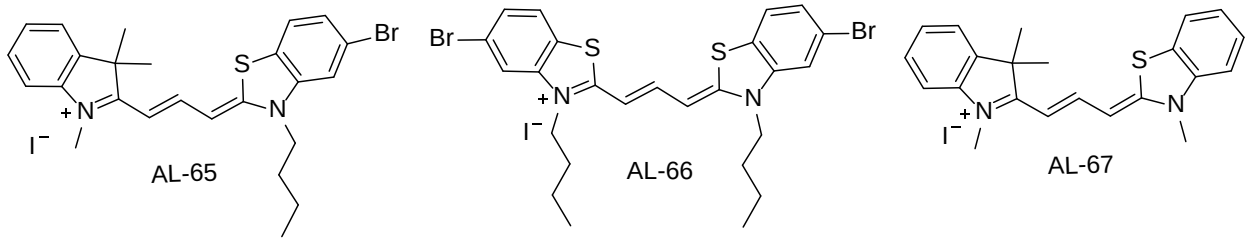

Figure 2.1 Structures of novel cyanine dyes

Due to the nature of the residues present in the sites of interest on their protein, it is expected that the dye with the most hydrophobic moieties will show preference in binding with bovine serum albumin thus supporting their potential use for applications requiring the non-covalent labeling of proteins.

2.2 Experimental

2.2.1 Instrumentation and software

All absorbance measurements were performed using a Cary UV/VIS/NIR (Lambda 50) Double Beam Spectrophotometer (Norwalk, CT) performed in 1.0 cm quartz cuvettes (Starna Cells, Atascader, CA). All fluorescence measurements were performed in 1.0 cm cuvettes using an ISS K2 spectrofluorometer and all samples were excited using a LaserMaxx laser (Rochester, NY) at appropriate wavelengths. All spectral and data analyses were processed and evaluated via Microsoft Excel 2007.

2.2.2 Solvent selection and sample preparation

Specifications regarding sample solubility and pH are also necessary factors that need to be addressed. For these experiments, liquid samples were selected as the suitable physical state of the dye and further methods of sample preparation were based on this selection. In the case of dye protein interactions, a suitable solvent system would be one in which the dye and protein dissolve without denaturing the protein. Because the dyes vary in structure, initial dye dissolution and spectral behavior in an appropriate solvent was evaluated systematically through absorbance spectroscopy by way of molar absorptivity and aggregation behavior. For characterization experiments, solvents were selected based on dye solubility and material availability. To simulate physiological conditions, experiments regarding dye interactions with

BSA would need to be carried out in an aqueous buffer solution at pH 7.4. It should be mentioned that a saline-free aqueous buffer would further prevent the protein from "salting-out" of solution also. This requirement makes the initial dissolution of the solid dye a crucial factor to avoid precipitating the more hydrophobic dyes.

2.2.2.1 Dye solution preparation

Standard dye Nile Red was provided by Kodak (Rochester, NY) and novel dyes **AL-65**, **AL-66**, and **AL-67** were provided by the lab of Dr. Maged M. Henary; synthesized by Andrew Levitz (Georgia State University). A suitable mass of each dye was weighed directly into an 8 mL amber vial to prevent photodegredation and dissolved in ≥99.9% methanol provided by Sigma-Aldrich (St. Louis, MO) to prepare stock solutions to a final concentration of 1.0 mM. Each solution was sonicated for 5-7 minutes to assist with dye dissolution. From these stocks, working solutions were prepared by adding an appropriate volume of dye into a small portion of solvent in a 5 mL volumetric flask. The remaining amount of solvent was added to the mark and the solutions were vortexed for 30 seconds each. Working solutions were prepared in ≥99% methanol to a final concentration of 0.10 mM.

2.2.2.2 BSA solution preparation

Stock solutions of BSA (provided by Sigma-Aldrich, St. Louis, MO) were prepared to 1.0 mM by dissolving an appropriate mass of solid serum albumin in saline-free phosphate buffer solutions (referred to here on out as PBS) at pH 7.4. Working stock solutions for all binding studies were prepared to 0.10 mM by adding an appropriate volume of stock solution to a 5 mL volumetric flask, and diluting the sample by filling the flask with 3x distilled NanoPure water (Bernard Model D4751 ultrapure water system) up to the mark.

2.2.3 Determination of molar absorptivity

To obtain quantitative information regarding dye behavior and the extent of its interactions with bovine serum albumin, various methods have been reported in literature for these determinations. For quantifying the absorptive and emissive behaviors of cyanine dyes, the molar absorptivity and quantum yield are two specifications that are typically employed.

Referring back to Beer's Law, the relationship between absorbance, concentration, and molar absorptivity is described.

$$A = \varepsilon bc \qquad (17)$$

Spectroscopic measurements can be made to determine the molar absorptivity of a given substance: as the concentration of a solution increases, there should be a subsequent increase in absorbance. Furthermore, the absorbance can be plotted as a function of concentration wherein Beer's Law can then be fit to a linear equation, thus yielding a straight line; the slope of which is the molar absorptivity.[8]

2.2.3.1 Molar absorptivity sample preparation

A serial dilution of each dye was prepared in methanol at concentrations ranging from 1.0 – 5.0 μM. Absorbance measurements of the standard dye were taken before and after each novel dye to ensure a consistent instrument response. Each dye was analyzed simultaneously alongside Nile Red and replicated at least three times to ensure reproducibility. Microsoft Excel 2007 was used for all linear regression analyses from which the slope of the absorbance units as a function of concentration were obtained.

2.2.4 Determination of quantum yield

The quantum yield of a compound is the rate of emissive processes compared to the rate of absorbed processes, or simply the number of photons emitted versus the number of photons

absorbed.[27] Various methods of quantum yield determinations exist with the two most prevalent techniques being the photon counting method or the comparative method.[27] The latter method is a simplistic approach that utilizes a standard compound with a known quantum yield with an absorbance and emission maximum wavelength (λ_{max} and Em_{max} respectively) near that of the unknown compound (Equation 18).[27] The determination of the unknown quantum yield can be found according to:

$$\Phi_S=\Phi_{STD}\left(\frac{slope_S}{slope_{STD}}\right)\left(\frac{\eta_S^2}{\eta_{STD}^2}\right) \qquad (18)$$

where Φ_s and Φ_{STD} are the quantum yields of the unknown and standard compound respectively and η is the index of refraction of the respective solvents. The comparative method was chosen for these experiments due to the availability of laboratory resources.

2.2.4.1 Quantum yield sample preparation

Serial dilutions of each dye for all absorbance measurements were prepared in methanol at concentrations ranging from 1.0–5.0 μM and all fluorescence measurements were taken at concentrations diluted 50 fold from the absorbance concentration values. Suitable concentrations for each dilution were determined based on instrumental limits for both absorbance and emission measurements, wherein measured absorbance values did not exceed 1.0 absorbance unit and absorbance values for fluorescence samples were kept below 0.10 units to avoid self quenching in what is known as the inner filter effect. The comparative method was used for the determination of all quantum yield values as given in (18), wherein the slope of the line obtained from the graph of the emission peak area as a function of absorbance units for each dye was used.

2.2.5 Aggregation studies

The aggregation properties of cyanines are important factors when considering a dye for protein binding applications as dye aggregation can affect the spectral behavior of the dye as well as its function *in vivo*.[12, 16] As a way of modeling the dye's transition from an environment similar to physiological conditions to a more hydrophobic environment such as one that could be encountered at BSA binding sites, the dyes were studied in a mixed solvent system. Furthermore, as Kim points out, various orders of aggregation can be observed, wherein the H-aggregated form can be dimeric, trimeric, and so on.[16] The resultant aggregation can be interpreted spectroscopically according to the following specifications: H-aggregation is signified by a blue shifted absorbance peak relative to the primary monomer band, while J-aggregation is signified by a red shifted peak relative to the monomer band.[12] As mentioned previously, cyanine dye aggregation can be induced by variances in its immediate microenvironment. Additionally, this behavior has been used as a detection system for proteins or other specified molecules in question. Depending on the application and the type of detection required, dye aggregation can be beneficial or disadvantageous to the application. In terms of non-covalent labeling, an increase in the dye's fluorescence signal upon binding with the protein would be useful for ultra-trace detection. Because H-aggregates tend to be weaker in fluorescence than J-aggregates and the monomer form of the dye, therefore, minimizing H-aggregation would be preferable for fluorescence detection.

2.2.5.1 Aggregation sample preparation

The aggregation behavior of the dye can be tested by adding a constant concentration of dye to PBS and increasing the amount of methanol in a series of dilutions. Samples were

measured by increasing the percent of methanol of the dye in pH 7.4 saline free PBS until no discernible changes were observed.

2.2.6 Determination of binding stoichiometry

An important parameter for supporting binding interactions is that of the Job's Plot. This technique uses the method of continuous variation in dye and protein ratios to determine the stoichiometry of the predominant complex if multiple interactions occur.[8] This is true with cyanines and proteins as according to Tatikolov and coworkers who observed complex binding interactions with cyanines and proteins.[28] Their work describes the potential of multiple forms of the dye to binding to the protein.[28] Thus, determining binding ratios could uncover the stoichiometry of the dominating complex and allow for the determination of binding constants of those complexes. This method involves varying the ratio between the dye and protein solutions, while keeping the total concentration of the solution constant. Fluorescence spectroscopy can be used to verify the ratio of the dominating complex as indicated by the highest point of emission intensity as a function of the mole fraction of the protein.[8]

2.2.7 Determination of the binding constant

Two variations of the Scatchard method as a shown in (14) and (16) were used for determining binding interactions between the novel dyes and BSA. A series of samples were prepared in PBS at pH 7.4 containing an appropriate constant concentration of dye with increasing amounts of BSA in micromolar concentrations. Both absorbance and fluorescence measurements were performed and samples were prepared with respect to the necessary specifications of each instrument.

2.3 Results and discussion

2.3.1 Spectroscopic characterization of trimethine dyes

2.3.1.1 Molar absorptivity analysis

Spectroscopic analyses determined the absorbance maxima (λ_{max}) and molar absorptivities (ε) of the trimethine dye series. As expected, there was a linear increase in the absorbance of each dye (Figure 2.2a – c) as their concentrations were increased, thus confirming their adherence to Beer's Law. A plot of the dyes' concentrations as a function of absorbance at their λ_{max} values (Figure 2.3) show that **AL-65** had the highest average molar absorptivity at 550 nm while **AL-66** had the lowest at 566 nm. **AL-67** displayed an absorptivity value in between the two with a maximum absorbance value at 542 nm. A summary of the average molar absorptivities are given in Table 2-1.

An examination of the absorbance spectra show that each dye primarily exists in its monomer form as evidenced by the prominent monomer or M-band. Moreover, the blue shifted shoulder peak to the left of the M-band indicates the slight formation of H-aggregates, which is most notable for dyes **AL-65** and **AL-67**. Dye **AL-66** appears to show a sharper monomer band compared to the other dyes. This is thought to be related to the polarity of the solvent in comparison to the structure of the dye. The butyl substituents add to overall hydrophobic character of the dye. Given that **AL-67** does not contain this group, it would display more aggregation in a less polar solvent.

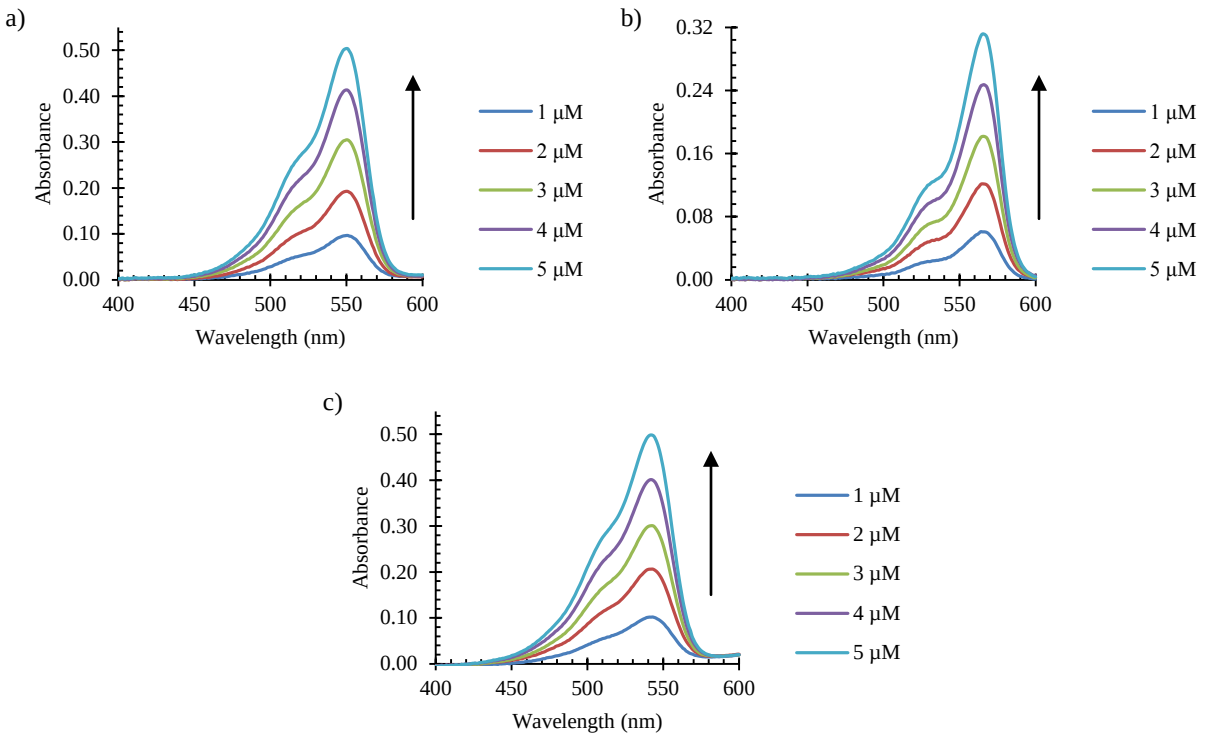

Figure 2.2 Absorbance as a function of wavelength of trimethine dyes in methanol a) AL-65 b) AL-66, c) AL-67

It can be observed that the molar absorptivity of **AL-66** was lower than the other dyes in methanol despite its monomerization in methanol. Despite remaking stock solutions and repeating the experiments, the value still remained low. This value could be attributed to the purity of the dye or an error in the preparation and dissolution of the samples. The later explanation could have resulted in lower concentrations of dye, thus lowering their absorbance values.

Furthermore, dye **AL-67** showed the second lowest molar absorptivity value, which can be attributed to the dye's structure which allows more of the dye to remain in its aggregated form, thus lowering the absorbance values of the monomer form. Referring back to Beer's Law, the decreased concentration of monomer forms of the dye in solution would lead to a decrease in the in absorbance values, which is proportional to the molar absorptivity.

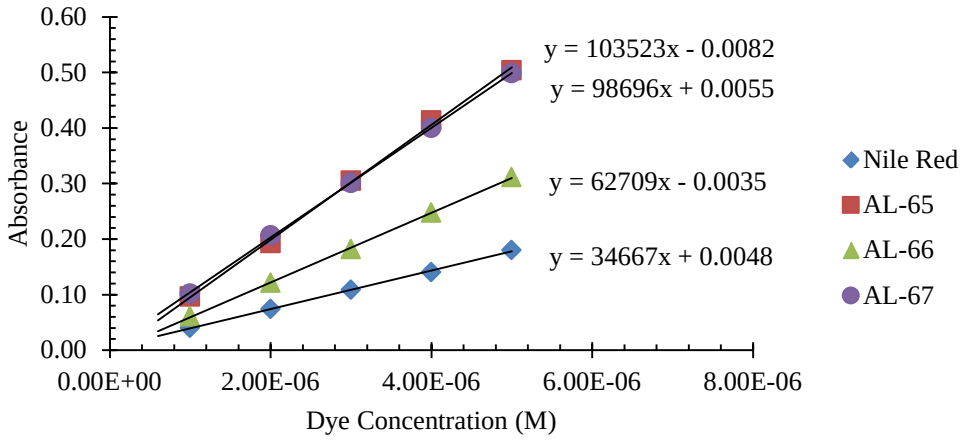

Figure 2.3 Absorbance as a function of concentration of trimethine dyes in methanol

Table 2-1 Average molar absorptivities of trimethine dyes

Dye	λ_{max} (nm)	Avg. ε ($M^{-1}cm^{-1}$)	Std. Dev.	%RSD	Replications
AL-65	550	1.03E+05	5.64E+02	0.547	3
AL-66	566	6.23E+04	1.14E+03	1.835	3
AL-67	542	9.78E+04	1.01E+03	1.030	4

2.3.1.2 Quantum yield analysis

The quantum yield of each dye was compared to the value of Nile Red in methanol (Φ = 0.70). A summary of the results are shown in Table 2-2. **AL-65** displayed the highest emission intensity of all three dyes with an emission maximum (Em_{max}) at 576 nm, followed by **AL-66** at 588 nm, and then **AL-67** at 570 nm (Figure 2.4a – c). It can be observed that the fluorescence intensity of each dye increased as a function of its concentration with good linearity (Figure 2.5a – c). As expected, the emission spectra were a mirrored image of the absorbance spectra, with the H-band displaying weaker fluorescence intensity than the monomer band, which is clearly seen in the spectra and correlates with results described in the literature; wherein H-aggregates tend to have lower quantum yields.[16]

Dye **AL-66** displayed the highest quantum yield compared to the other dyes; though it did have the lowest molar absorptivity. Based on the definitions of these parameters, this dye has a low light absorbing ability when compared to the other dyes, but a higher rate of radiative processes than the other dyes. A study conducted by Levitz and coworkers mention that cyanines containing heterocycles substituted with bromine atoms experience what is called the heavy atom effect, which in turn leads to an increased quantum yield.[29] This is further supported by the evidence showing that **AL-65**, containing one bromine atom had a higher average quantum yield value than **AL-67** which had the lowest average quantum yield value of all of the dyes.

Again, much like in the absorptivity measurements, the structure of **AL-67** would aggregate more in the less polar methanol, thus leading to a lower emission intensity of the monomers in solution.

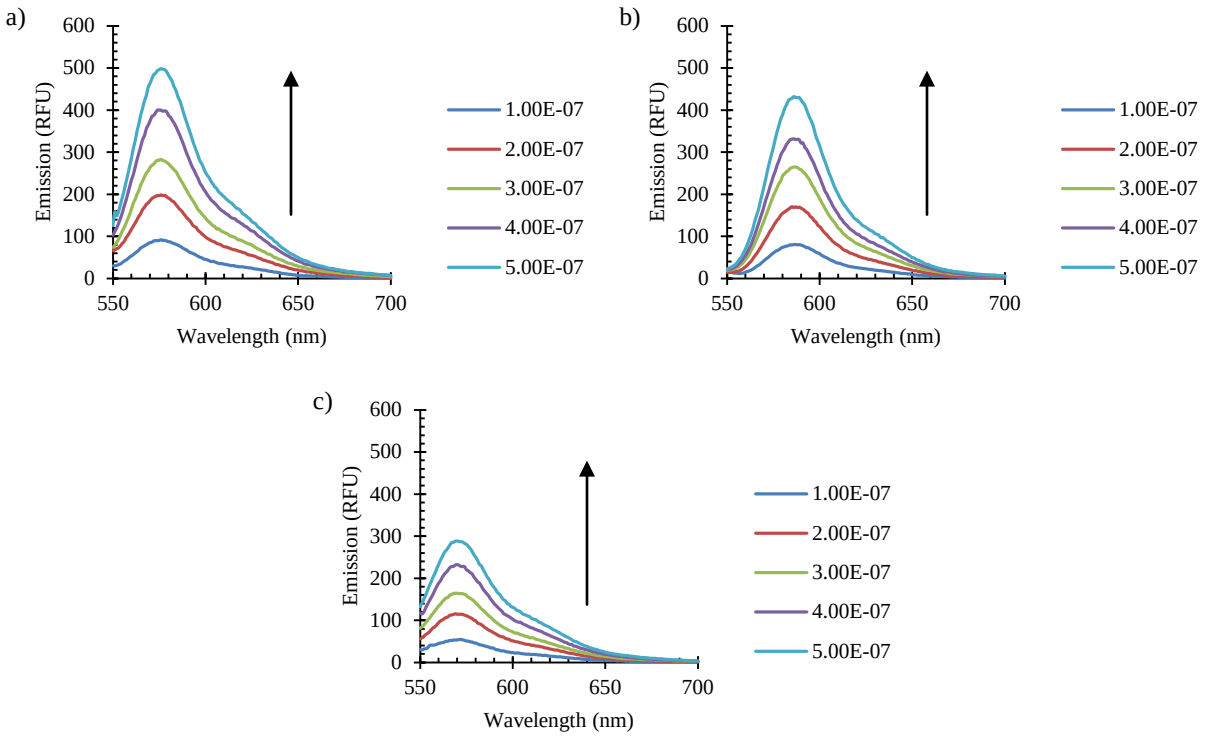

Figure 2.4 Emission spectrum of novel trimethine dyes in methanol a) AL-65 b) AL-66 c) AL-67

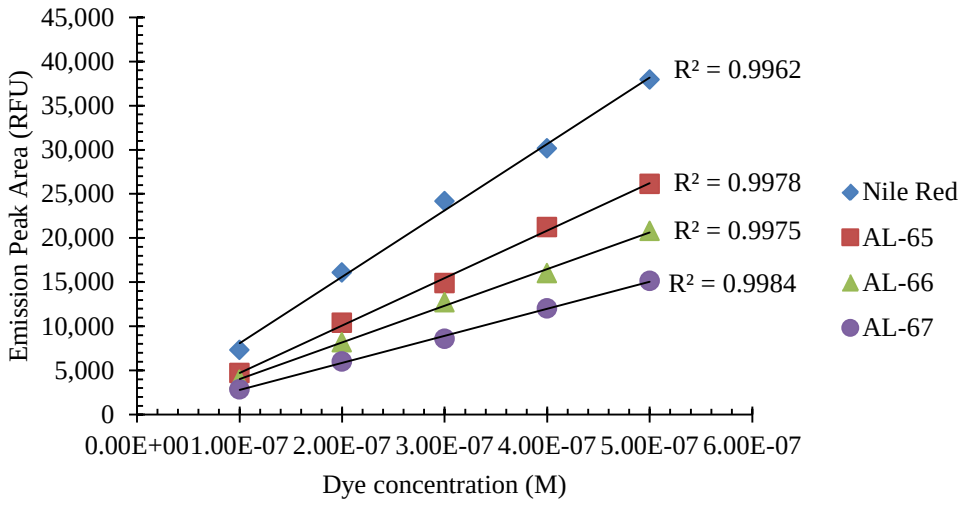

Figure 2.5 Emission peak area as a function of trimethine dye concentration

Table 2-2 Average quantum yields of trimethine dyes

Dye	λ_{max} (nm)	Em_{max} (nm)	Stoke's Shifts (cm^{-1})	Φ	Std. Dev.	%RSD	Replications
AL-65	550	576	821	0.15	0.017	11.42	2
AL-66	566	588	661	0.22	0.015	6.80	2
AL-67	542	570	906	0.10	0.008	7.63	2

2.3.2 Aggregation behavior

Furthermore, the aggregation behavior of each dye was studied in a varied solvent system made from a series of buffer solutions increasing in percent methanol from until no discernible changes were observed. An examination of the dye spectra shows the changes in dye aggregation behavior in a more polar environment to that of a more non-polar environment (Figures 2.6, 2.7, and 2.8). At 1% methanol, dye **AL-65** remained primarily in its monomer form with a λ_{max} at 546 nm. The dye also showed some evidence of a higher order of aggregation as denoted by the very weak redshifted peak with respect to the primary M-band. As the percentage of methanol increased, there was noticeable disaggregation along with a 4 nm redshift in the M-

band to 550 nm. This behavior can be attributed to the presence of the hydrophobic butyl side chain that would cause the dye to self-associate in the aqueous buffer.

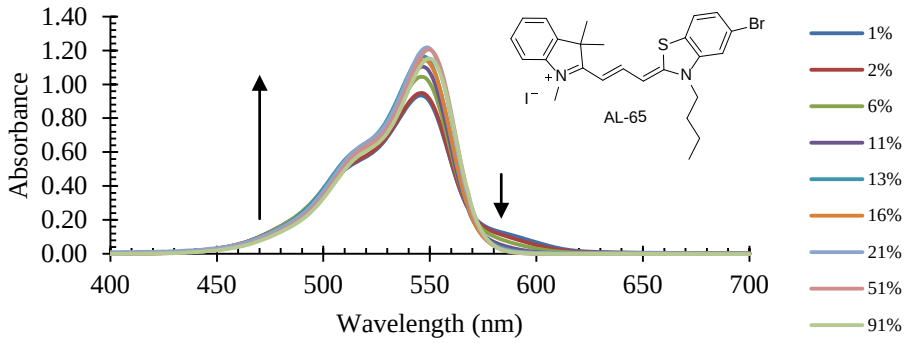

Figure 2.6 Aggregation behavior of AL-65 in PBS with increasing percent methanol

Further supporting the suggestion of hydrophobic driven self-association is the spectral behavior of **AL-66** which shows a dramatic increase in monomerization with increased methanol percentage. In a more aqueous environment, the absorbance spectra of **AL-66** (Figure 2.7) show weak and broadened bands with little definition which can be attributed to the many electronic transitions of the various aggregated forms of the dye. When the percent of methanol in the solution was a 16%, there is a noticeable recovery of the monomer band at 566 nm that increases dramatically as the percent of methanol reached 91%.

Additionally, it should be mentioned that the dye solution at 1:99 (%v/%v) in methanol and PBS, the sample initially gave off a pale purple color. However, upon increasing the percent of methanol, the solution turned a bright pink.

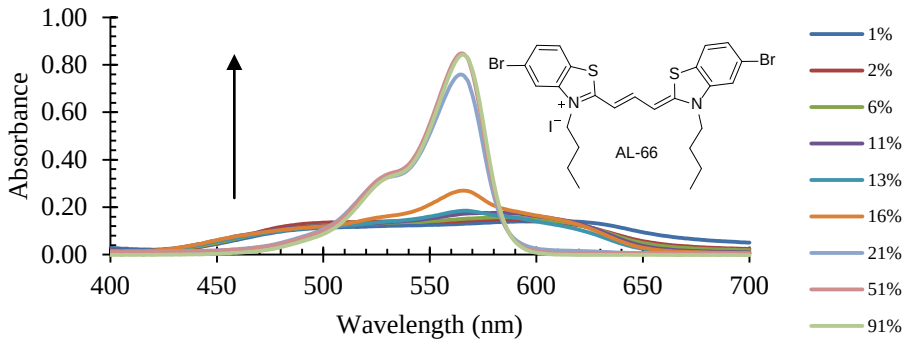

Figure 2.7 AL-66 in PBS with increasing concentration of methanol

This color change is also similar to results observed by Sun and coworkers wherein the various aggregates of a cyanine dye were shown to produce various colors.[17] As mentioned previously, the target sites for binding on BSA are the ones containing hydrophobic residues. These results suggest that dye **AL-66** could possibly display the same behavior in this environment rather than the aqueous environment of the buffer solution. It should be noted that the behaviors of the dyes were studied at 76 and 81% methanol, however, there was observed turbidity in the solution for all three dyes. This could be attributed to the concentration of buffer wherein the presence of the dye may have caused precipitation of the buffer. Dye **AL-67** showed no apparent aggregation or disaggregation, as there was no noticeable trend in the monomer absorption bands at 542 nm. This is more than likely due to its preferential solubility in more polar environments; however, the H-band indicates that some of the dye was still in its aggregated form in both the polar and less polar solvent.

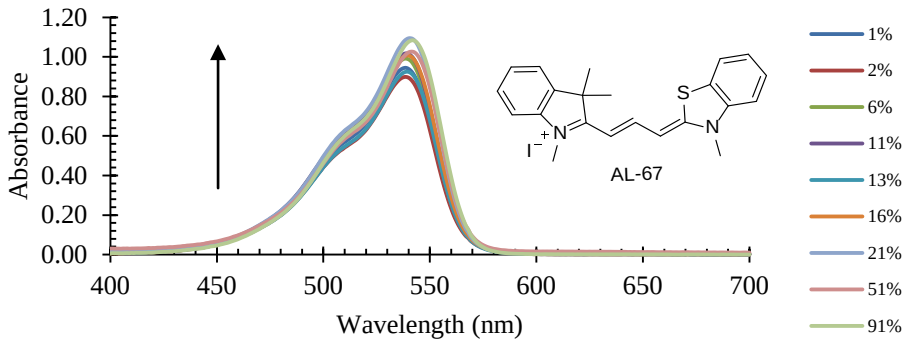

Figure 2.8 Absorbance as a function of wavelength for novel trimethine dyes in PBS with 1 – 100% methanol

The aggregation studies show that when in more hydrophobic environments, dyes **AL-65** and **AL-66** tend to aggregate less in more hydrophobic environments. This suggests that when encountering that of the hydrophobic binding pockets of BSA, both dyes will remain in their monomer form, thus preventing the undesirable aggregation.

2.3.3 Binding behavior with cyanine dyes and BSA

2.3.3.1 Absorbance measurements

The binding interactions between the novel trimethine dyes and BSA were also investigated. Dyes **AL-65** and **AL-67** showed no consistent spectral trends upon addition of BSA in micromolar concentrations (Figure 2.9a and b).

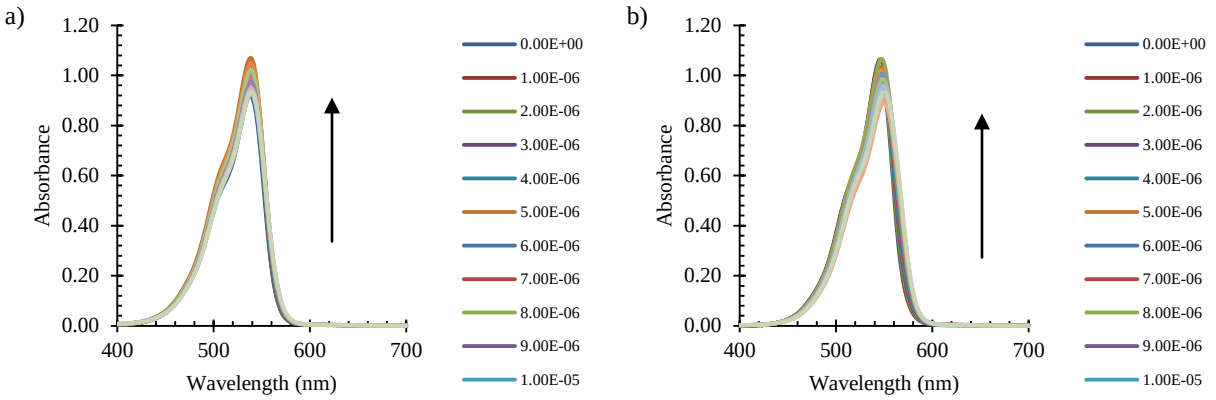

Figure 2.9 a) AL-65 and b) AL-67 with increasing concentration of BSA from 0 – 20 µM

The most significant spectral changes occurred with dye **AL-66**. A qualitative analysis of the spectra provides information regarding what kinds of interactions could be occuring. It can be observed in Figure 2.10, that the dye experienced a combination of monomerization and aggregation in PBS before any protein was added. The most prominent aggregation is presumed to be J-aggregation due to its red shift in wavelength in comparison to the primary monomer band at 566 nm.

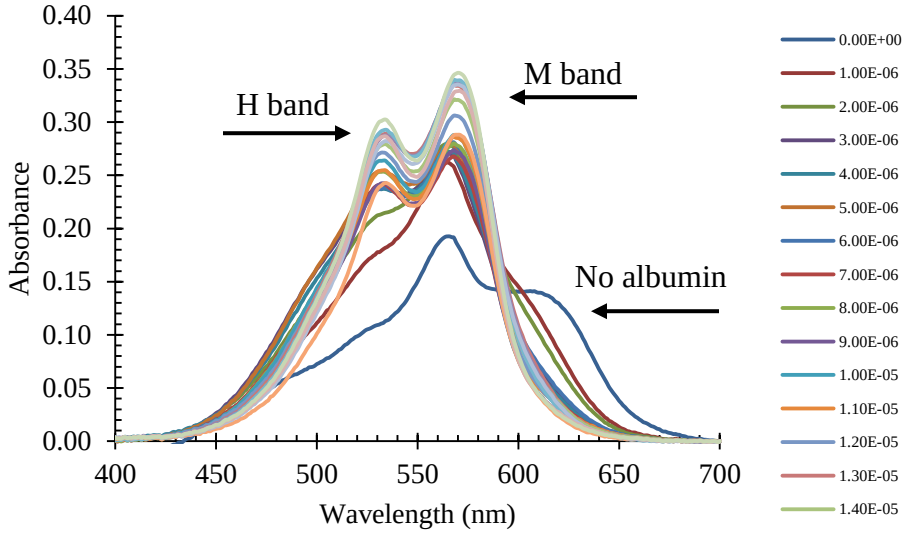

Figure 2.10 Absorbance as a function of wavelength of 10 AL-66 with increasing concentration of BSA from 0 – 20.0 µM in PBS pH 7.4

Upon addition of BSA, there was a concomitant increase in both the monomer and aggregation bands; however the newly observed aggregation was H-aggregation as noted by its blue shift with respect to the monomer band at 533 nm. It can be observed on a plot of the absorbance as a function of protein concentration (Figure 2.11 a and b) that the monomer absorbance increaseases slightly with a maximum absorbance at 566 nm, while we see the J-aggregate peak decrease while the H-aggregate peak increases. As varying orders of aggregation can be observed spectroscopically, it can be seen that dimer band of the dye sharpens as the concentration of protein is increases.

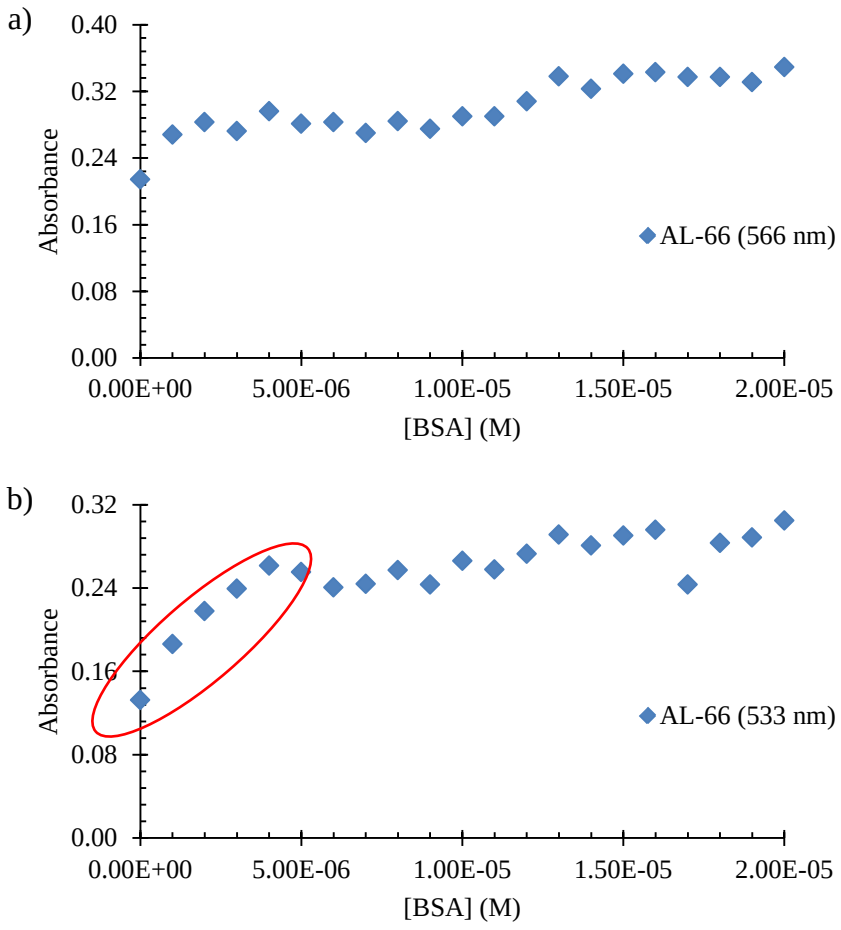

Figure 2.11 a) Absorbance as function of [BSA] for dye the monomer band of dye AL-66,bsorbance as a function of [BSA] for dye the dimer form of AL-66 at 533 nm.

Furthermore, the absorbance of the dimer peak gives what appears to be a linear increase in absorbance from 0 – 5.0E-06 M of BSA. To examine this increase further, additional experiments were carried out with specific focus on the dimer band at 533 nm over the abovementioned range to further investigate a potential linear dependency (Figure 2.12 and 2.13). However, results did not yield ideal linear plots for these experiments despite repeated attempts. However, there are still variances in dye monomerization and aggregation as seen in the previous data.

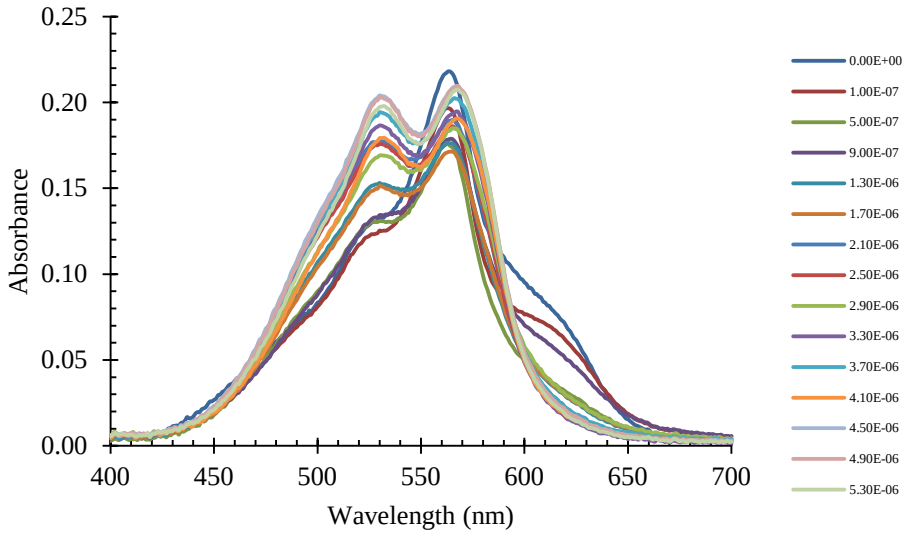

Figure 2.12 AL-66 in PBS with increasing BSA concentration over 0 – 5 µM protein.

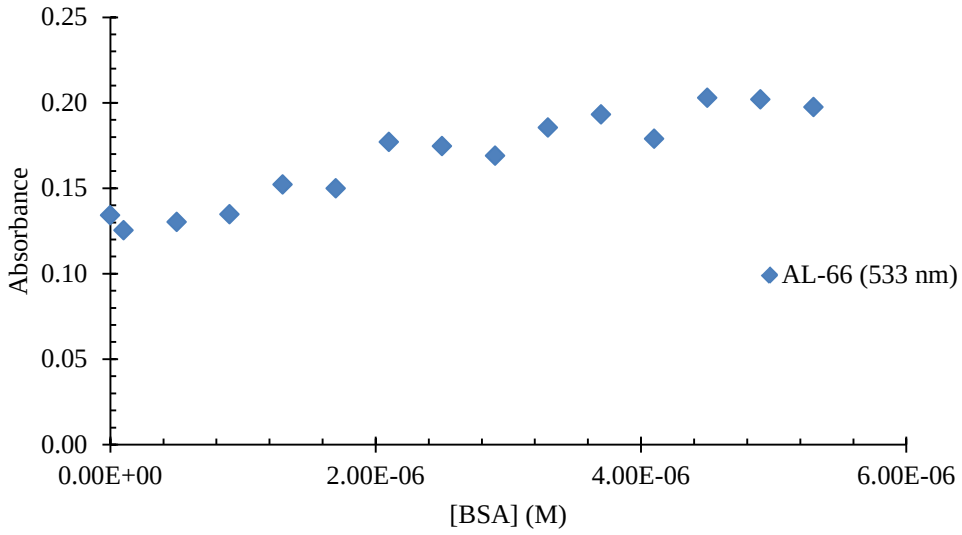

Figure 2.13 Absorbance of AL-66 at 533 nm as a function of BSA concentration

Given the structure of **AL-66** and the target binding pocket of BSA, it is not surpring that the dye binds in such manner. As its interactions with the binding site would be governed by hydrophobic interactions, it can be inferred that the dimer form of the dye is more hydrophobic than the monomer form, which would in theory, be more suitable for binding.

An analysis of the equilibrium parameters of this system appears to be more complex than the average 1:1 binding typically observed with cyanines and serum albumins. Kim mentions that absorbance values can be used to calculate association constants if there is a significant difference between the primary absorption band of the free dye and the bound dye.[16]

However, using Beer's Law, some quantitative information can be deduced by obtaining the molar absorptivity of the dyes. Therefore, an additional series of experiments were carried out and the molar absorptivities of each dye were determined in PBS as shown in Table 2-3, and Figures 2.14 and 2.15.

Table 2-3 Average molar absorptivity values of trimethine dyes in PBS

	Nile Red	AL-65	AL-66	AL-66 (533)	AL-67
ε ($M^{-1}cm^{-1}$)	3.83E+04	1.10E+05	8.11E+04	4.44E+04	1.04E+05

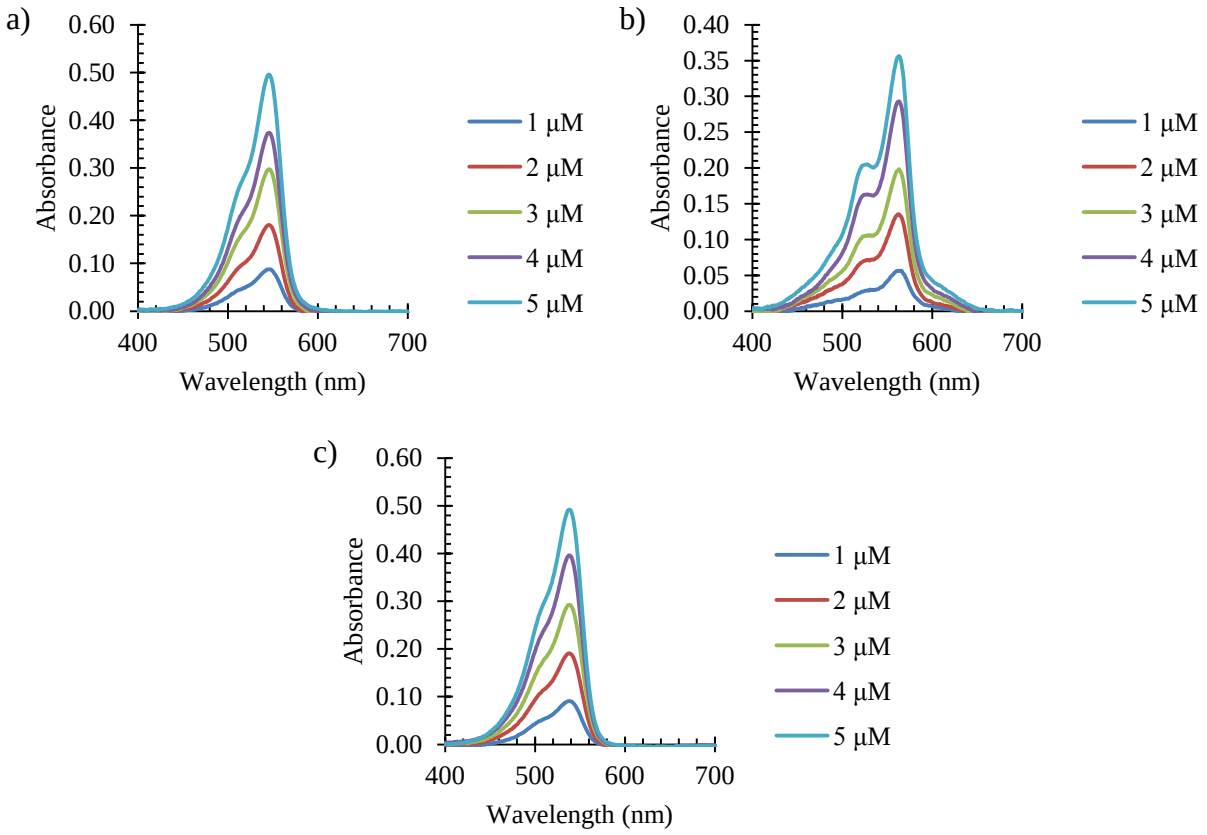

Figure 2.14 Absorbance as a function of wavelength of AL-65, AL-66, and AL-67 in PBS.

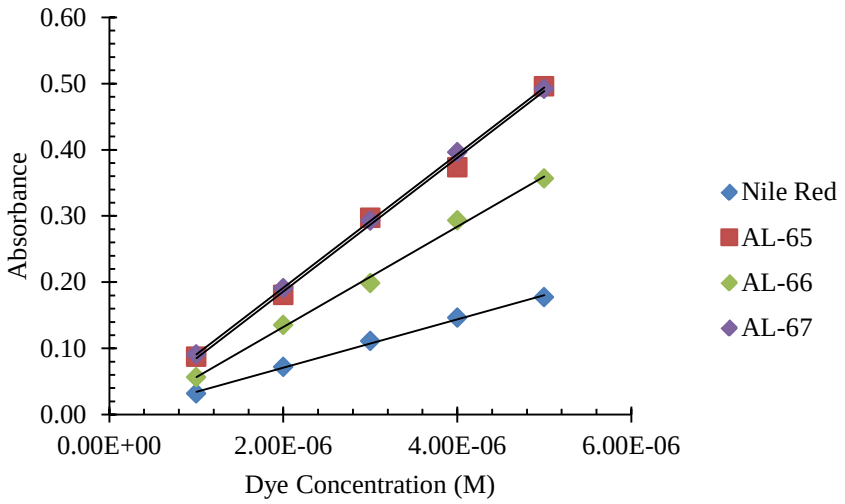

Figure 2.15 Absorbance as a function of dye concentration for novel trimethine dyes in PBS

In PBS, **AL-66** gives a primary monomer band at 563 nm with a sharpened H-band and a very weak J-band. In the presence of BSA in PBS, the monomer band experiences at 2 nm redshift. Using the information gathered from the dye in the PBS, the molar absorptivity of the dye in its monomer form can be determined. It should be noted that during the experiments, dye **AL-66** was prone to aggregate in solution if the sample was not shaken thoroughly to mix. This could be an explanation as to why a linear dependency was difficult to obtain in the previous experiments with BSA (Figures 2.12). Furthermore, when applied to Beer's Law, the concentration of dye bound and free can be determined.

The obtained molar absorptivity of the monomer form of **AL-66** had an average value of 8.11E+04 $M^{-1}cm^{-1}$. Using this obtained value, we can calculate the concentration of the monomer form of the dye. Based on the peaks observed in the spectra, if it is assumed that whatever concentration of dye is not in the monomer form, what remains is in some aggregated state. Furthermore, the molar absorptivity of the band at 533 nm was also determined with a value of 4.44E+04$M^{-1}cm^{-1}$.

This low value is expected given the weak aggregation band. Using these values, it is possible to obtain dye concentrations of both of the forms present in the spectra of the dye in the presence of containing BSA under the following assumptions: If it is assumed that all of the bound dye is in its dimer form, the concentration of the dimer can be calculated and any other form of the dye (whether it be monomer or another order of aggregation) is considered to be unbound. A Scatchard plot can be used to obtain equilibrium information between the two forms of dye in the presence of BSA (Figure 2.16) as described in (14). An equilibrium constant of 1.61E+06 was obtained from the slope of the equation of the line.

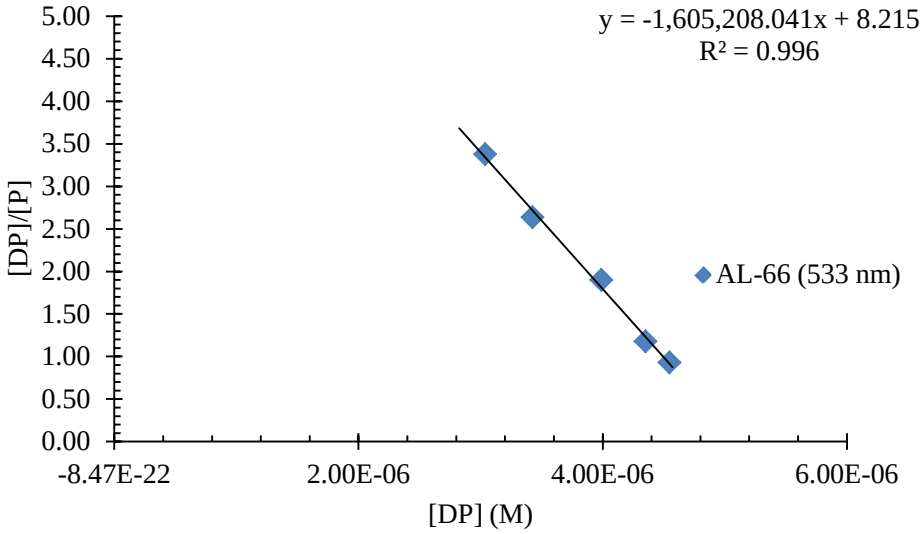

Figure 2.16 Scatchard plot of AL-66 at 533 nm.

It should be noted that this value simply describes the state of this system in accordance with the concentrations of the different forms of the dye. More thorough studies would be needed to deduce the specific interaction regarding the dimer form of the dye and the protein. As stated before, the absorbance band of the bound and free forms of the dye would have to be a significantly different wavelength in order to determine a more accurate binding constant via

absorbance. Therefore, further studies were conducted to gather more information regarding the binding interactions between the species by way of fluorescence spectroscopy.

2.3.3.2 Fluorescence measurements

To further examine the nature of the dye-BSA interactions, fluorescence measurements were also performed. An analysis of the fluorescence data shows that all three dye experience and increase in intensity as the concentration of BSA increases, unlike the absorbance data. The dyes themselves showed very minimal fluorescence before the protein was added as well as a redshifted emission peak. It can be inferred that all three dyes do have some sort of interaction with the protein; however, they interact in different ways. The results for each dye are shown in Figure 2.17a – c.

In the case of **AL-65** and **AL-67**, there were no discernible changes in the absorbance spectra. However, there appears to be stabilization of the dye's polymethine chain as denoted by an increase in fluorescence intensity. As mentioned previously, the stabilization of the chromaphore can be enhanced by rigidization; not only in structure, but in environment as well. Therefore, it can be noted that while the dye shows no signs of aggregate binding, the monomer form of the dye could be stabilized by the protein, thereby increasing its fluorescence. While the binding location could not be determined from this data, it can be suggested that in lacking a more hydrophobic character, dyes **AL-67** more than likely binds in a region that is more hydrophilic than that occupied by **AL-66** or **AL-65**.

Referring back to the absorbance spectra, dye **AL-66** displayed increased H-aggregation as the concentration of BSA increased. As mentioned previously, H-aggregates are weakly fluorescent. However, an increase in emission intensity was observed with this dye, which could

suggest that the monomer form of the dye is still stabilized by the HSA. Thus a binding constant could be determined for the monomer form of the dye using the fluorescence data.

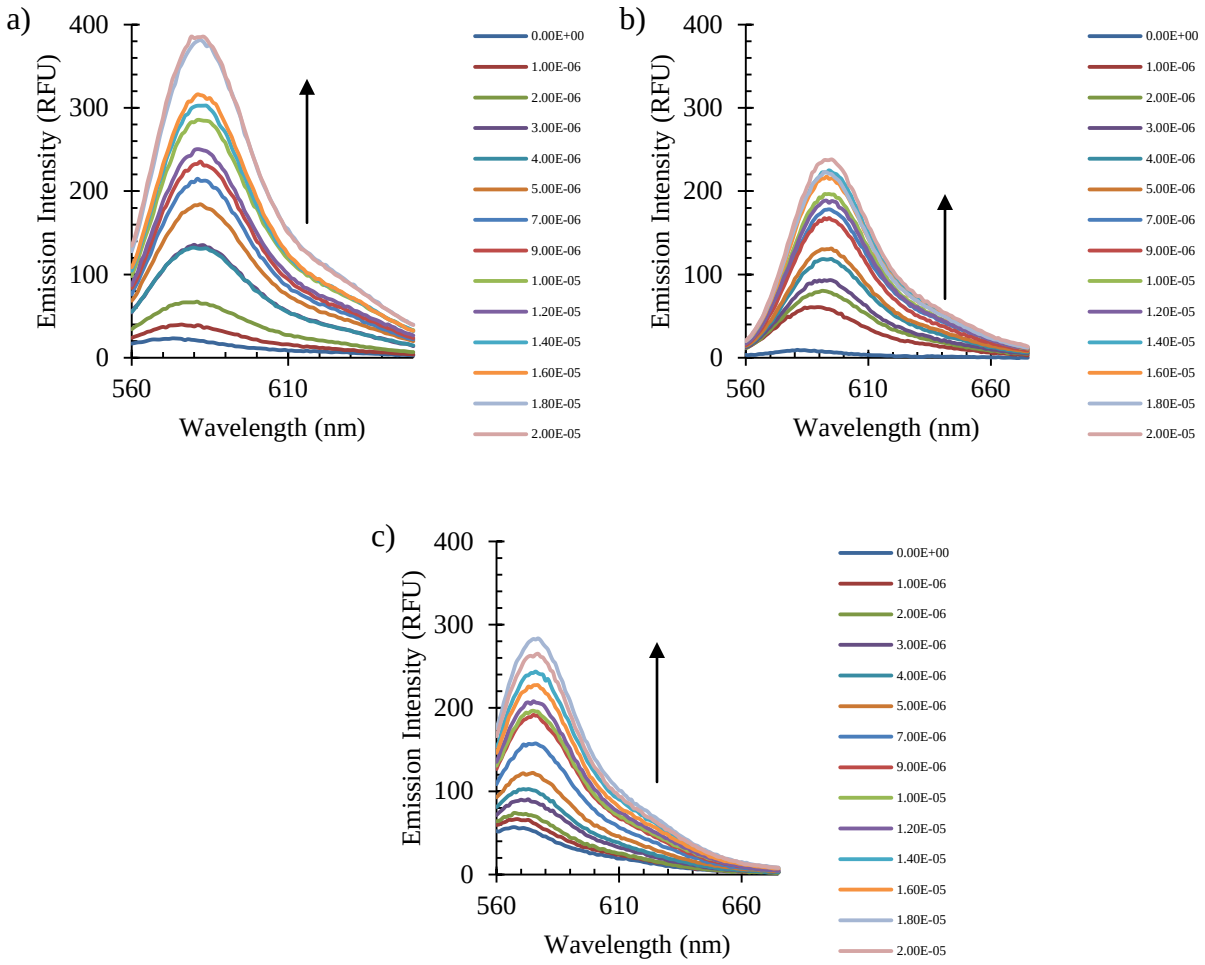

Figure 2.17 Emission intensity as a function of wavelength of cyanine dyes a) AL-65, b) AL-66, and c) AL-67 with increasing concentration of BSA.

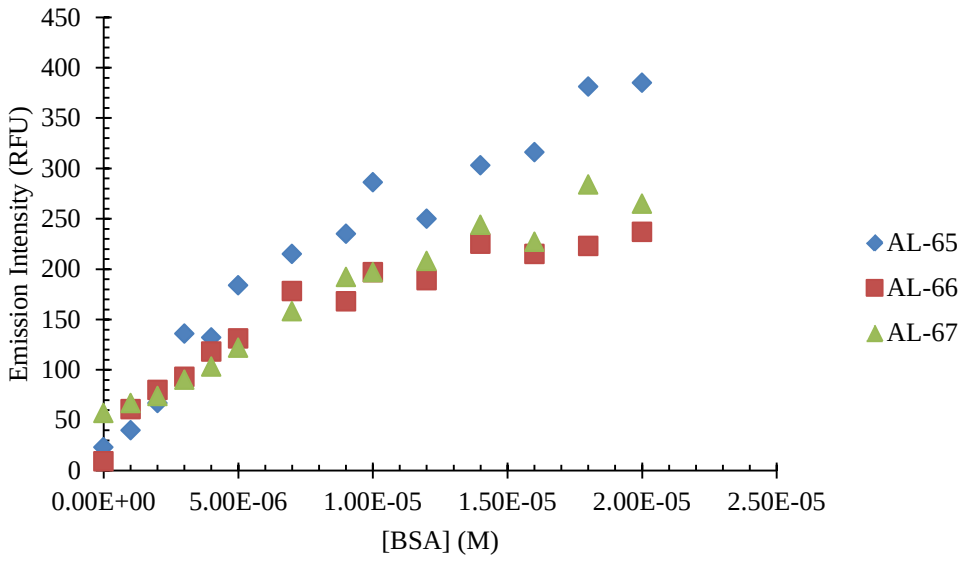

Figure 2.18 Emission intensity of trimethine dyes as a function of BSA concentration

A plot of the emission intensity versus the concentration of BSA (Fig. 2.18) shows that **AL-66** and **AL-67** have weaker fluorescence when interacting with the protein than **AL-65**. The modified Scatchard method (16) was used to determine binding information. The data show that **AL-66** has the highest binding constant, followed by **AL-65**. The results are shown in Table 2-4.

Table 2-4 Trimethine dye and BSA binding constants

AL-65	AL-66	AL-67
9.88E+04	1.20E+05	1.07E+04

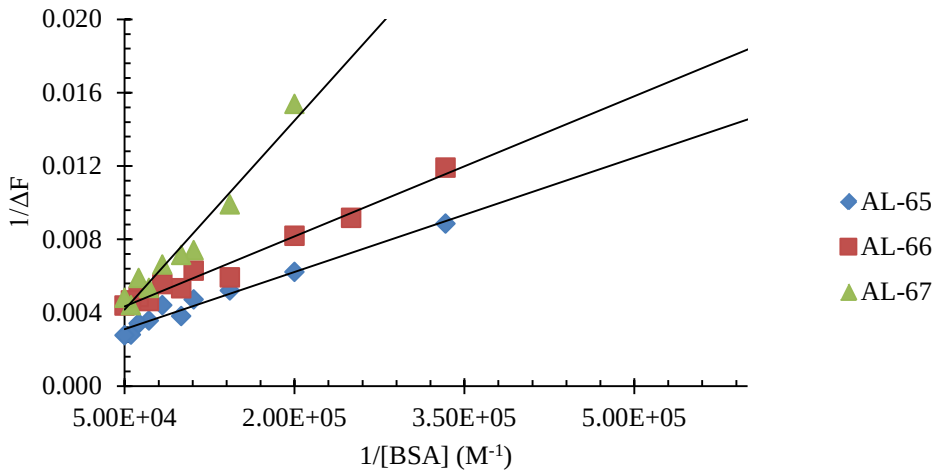

Figure 2.19 Scatchard plot of binding interactions between trimethine dyes and BSA

These results can suggest the different interactions that the dye may have based on its structure. As mentioned before, **AL-66** shows aggregation in the presence of the protein which could be due to the more hydrophobic nature of the dye with its butyl side chains. Furthermore, this form of aggregation is weakly fluorescent due to the nature of the molecular stacking. **AL-65** only contains one butyl side chain, which could interact with the protein as well, but not as strongly as **AL-66**.

2.3.4 Job's analysis

A Job's analysis was conducted on all three dyes via fluorescence spectroscopy and the results of the studies are shown in Figures 2.20 – 2.22.

Dye **AL-65** showed maximum fluorescence intensity at a BSA mole fraction of 0.5. This mole fraction corresponds to a 1:1 binding ratio, which as mentioned previously is typically seen with cyanines and proteins as mentioned by Beckford and Kim.[12, 16]

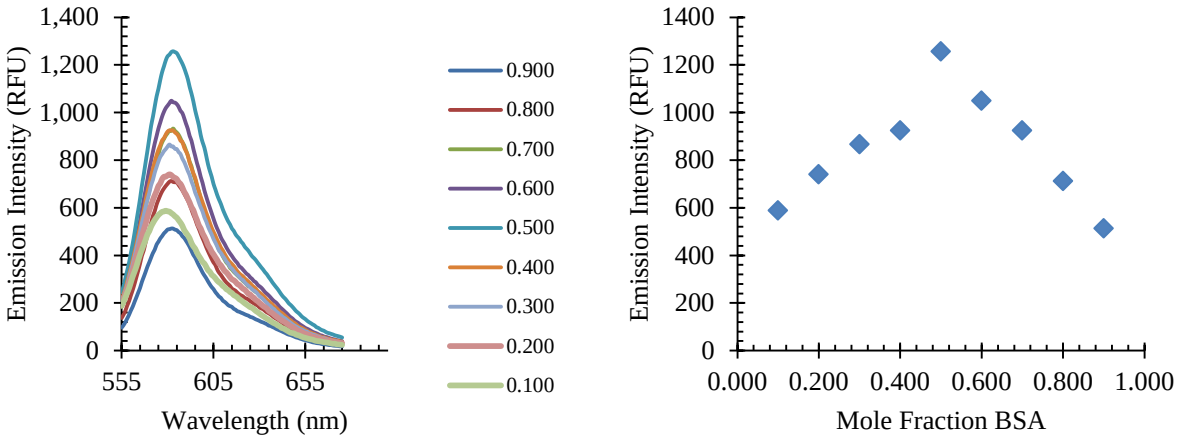

Figure 2.20 Job's analysis of AL-65 and BSA in PBS

Furthermore, **AL-66** also showed signs of binding in a 1:1 ratio. However, it should be mentioned that this only accounts for that of the monomer band. While it is possible that the dimer form could bind as well, the weakened fluorescence intensity of the H-aggregates, made anaylsis via emissions near impossible to accomplish. However, the binding analysis for the monomer itself is validated based on its 1:1 binding with the protein.

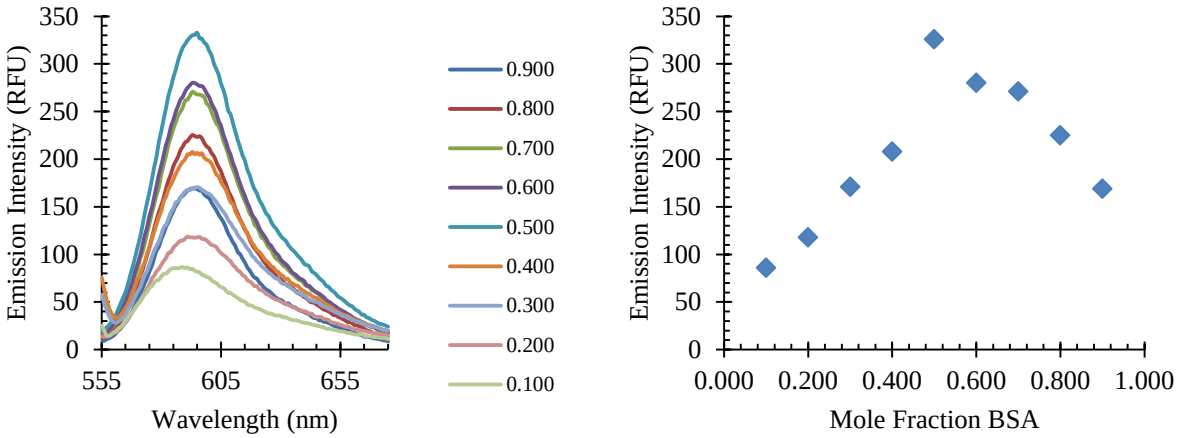

Figure 2.21 Job's analysis of AL-66 and BSA in PBS

Dye **AL-67** showed the most inconsistency in its Job's analysis. There was no clear increase point of maximum intensity for the various ratios studied. While the dye did show an

increase in fluorescence intensity, it may be that the dye was not hydrophobic enough to have an affinity for the targe binding sites.

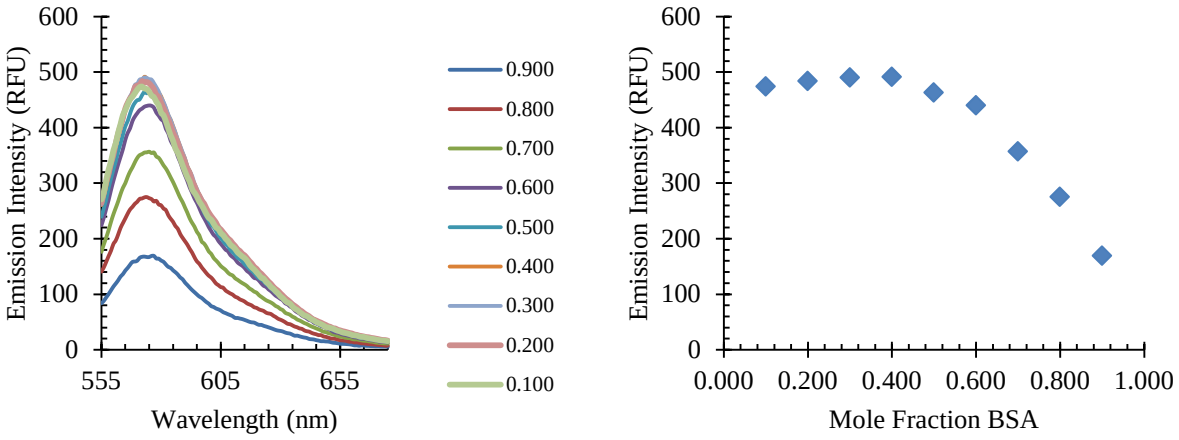

Figure 2.22 Job's analysis of AL-67 and BSA in PBS

2.4 Conclusions

A study was conducted to investigate the nature of the interactions between three novel cyanine dyes and bovine serum albumin to investigate non-covalent interactions and binding behaviors. Characterization results showed that the spectral behavior of the dye was dependent on its structure as well as its surrounding microenvironment which corresponds to results found in the literature. Dye **AL-65** was shown to have the highest molar absorptivity and a good quantum yield. It displayed minimal aggregation in buffer and an increased fluorescence upon interaction with BSA. These properties make it a good candidate for future labeling applications.

Dye **AL-66** displayed the most dramatic response to changes in the composition of its environment. The dye was shown to undergo significant aggregation in PBS and subsequent monomerization with increasing amounts of a more hydrophobic solvent. Furthermore, this dye also displayed the most spectrally dramatic interaction with BSA by self-associating in response to the protein.

An equilibrium constant was obtained to describe the system in terms of its monomer form and protein associated dimer form. These results show that an associated form of the dye is influenced by the presence of BSA; however alternative methods of measurement would need to be conducted in order to determine the true extent of their interactions and at which binding sites the interactions could potentially be occurring.

Furthermore, an analysis of the fluorescence data shows that there is some increased stabilization of each dye's monomeric fluorophores which lead to an increase in fluorescence intensity; however specific binding locations could not be certainly determined from this data.

AL-67 gave a moderately high molar absorptivity, but a low quantum yield in methanol. The dye showed minimal aggregation in buffer and in methanol which is desirable for labeling purposes. However, upon interaction with BSA, the dye displayed some fluorescence enhancement, however it may not have been hydrophobic enough to fully interact with the protein.

3 CYANINE DYE INTERACTIONS WITH HUMAN SERUM ALBUMIN IN AOT/*N*-HEPTANE/WATER SYSTEMS

3.1 Purpose of study

Examining the binding interactions between functional cyanine dyes and carrier proteins such as human serum albumin (HSA) are of great importance for various bioanalytical applications such as site specific tumor targeting and drug conjugation. The extent of these interactions are an important parameter for *in vivo* applications involving the distribution and elimination of the compound.[30]

As more dyes are being synthesized for such purposes, it is necessary to utilize different model systems for studying such interactions. More popular methods of studying dye and protein binding interactions show very promising binding data *in vitro*. However, very few studies have examined the nature of cyanine dye binding interactions with proteins under *in vivo* mimetic environments; specifically, that of biological membranes. It is well known that cyanine dyes are extremely sensitive to light and to changes in their immediate microenvironment; which thereby poses the question of whether the behavior of a dye in a bulk solvent would be different when compared to that of a more confined solvent system. Thus is it the goal of the following study to examine the binding interactions between a novel heptamethine cyanine dye and human serum albumin under bulk solvent conditions and biomembrane mimetic environments.

3.1.1 Proposed methods

The versatility of reverse micellar systems allows for the interactions between multiple species to occur in a confined chemical reaction space due to their internal aqueous core. These interactions include micellar catalysis, enzymatic reactions, and protein purification.[30] Additionally, these systems have been utilized for their solubilization characteristics and use in

the back extraction of proteins.[31] The most widely studied reverse micelle forming system is that of sodium dioctyl sulfosuccinate (AOT) in the presence of a non-polar solvent and water. Spectroscopic techniques such as those typically employed with *in vitro* binding studies will be used to compare the effect of the different environments on the dye and protein interactions.

3.1.2 The development and utilization of surfactant media

The study of surfactant micelles began with investigations of soaps conducted by McBain and coworkers in the early 1900s which made use of amphiphilic compounds called surfactants. These studies suggested the existence of a thermodynamically-stable liquid crystalline phase of these compounds. Further support of this media was found by Winsor and Luzzati through X-ray visualization; wherein the first depictions of such systems were presented in phase diagrams in terms of ternary composite mixtures containing a surfactant, a co-surfactant, and water.[32]

The most widely accepted model of micelles was that proposed by Hartley, wherein he described a spherical aggregate consisting of surfactant monomers whose hydrocarbon chains were arranged in such a way that minimized contact with any surrounding aqueous phases. Additionally, Hartley concluded that the formation of these structures was highly dynamic and that their rapid formation and dissociation implied a fluid nature due to the composition of the hydrophobic core compared that of the liquid hydrocarbon analogues.[32]

These early developments provided the bases for what is now known today: that surfactant micelles are thermodynamically stable structures composed of a hydrophobic core made from the extended alkyl surfactant chains, surrounded by hydrophilic headgroups.[32]

3.1.2.1 Specifics of reverse micellar systems

As more information was gathered about the formation of normal micelles, new studies incorporated the use of solvents varying in polarity, wherein the use of an apolar solvent system

gained much attention. Expanding on the works of alkylammonium salts by Batson and Kraus as well as alkylamine soaps by Hoerr and Ralson, Singeterry presented a list of micelle forming surfactants in non-polar solvents. These works determined that large organic cations and anions that are both highly soluble in the given solvent are too ionically associated to form micelles.[32]

The observations made by Hoerr and Schulman depicted a system incorporating water/potassium oleate/pentanol/benzene that gave a clear isotropic solution. The system contained large amounts of benzene and water (apolar and polar components) and small amounts of oleate and pentanol (soap/surfactant and co-surfactant respectively). The weight ratio of oleate to pentaol was kept within a narrow range. Initially, Schulman described this as an "oleopathic hydromicelle" whose formation and size was determined by the requirement that all of the surfactant mixture would be adsorbed at oil/water interface.[32]

Qualitative depictions of such systems were presented by Winsor which were inclusive of these apparent "reverse micellar" formations. The work of Ekwall and coworkers further demonstrated that a minimum amount of water was required for these structures for form. Much like their normal micellar counterparts, the incorporation of water along with the surfactant in an apolar solvent, the formation of stable near-spherical aggregates was observed. These structures were later referred to as "reverse micelles" and later coined "microemulsions" in regards to the observed phenomena; playing upon a smaller version of an emulsion droplet. These findings were confirmed by Friberg and coworkers, who found that Schulmans specifications in composition fell within the range of a thermodynamically stable solution region of the quaternary phase diagrams.[32]

Furthermore, Schulman also determined that a necessary condition in forming these microemulsions was that the surfactant (or surfactant mixture) have low solubility in the oil and

the water phase. Such a requirement would lead to zero interfacial energy during adsorption of the surfactant to the water droplets, wherein the zero interfacial energy would lead to an overall state of higher free energy. This is demonstrated by the fact that large amounts of water and oil containing surfactants form a three-phase equilibrium of near pure water or near pure oil. At the interface would be a highly ordered layer containing a liquid crystal of the ordered surfactant system. Variations in hydrocarbon chain length of the surfactant, the temperature of the solution and the oil/co-surfactant properties can create a disturbance in these phases, which lead to the formation of water/oil mixtures.

Ultimately, it was determined that the requirements to form highly concentrated water/oil mixtures are low equilibrium concentrations of the surfactant (or surfactant/co-surfactant) mixture in oil and water. This requirement reduces interfacial tensions to very low values (as stated above, zero interfacial energy yields the maximum free energy for the formation of a stable microemulsion. Additionally, high fluidity and flexibility of the surfactant membrane are also needed. The most highly studied of these systems was that of sodium dioctyl sulfosuccinate, more commonly known as Aerosol OT (AOT).

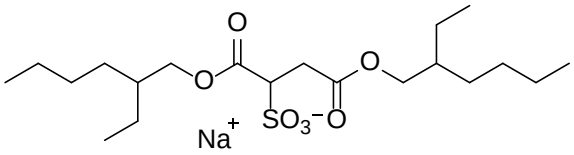

AOT

Figure 3.1 Structure of AOT

The determinations of reverse micelle formation and structure have been confirmed through the use of NMR and ESR through the use of order parameters and correlation times.[32] It

should be noted that these studies have also shown that in many cases, the formation of well-defined aggregates are not formed in typical microemulsions, wherein transitions between microemulsions and micelles could occur. Furthermore, the overall micelle itself would not be precisely spherical in shape.[32]

3.1.2.2 Cyanine dyes in reverse micellar media

While few studies have incorporated the use of cyanines in conjunction with proteins in reverse micelles, several studies have examined the behavior of cyanine dyes in these systems. Studies conducted by Nikolenko and coworkers showed that reverse micelles could act as "micellar sieves" for dye aggregate size control due to the ability to vary the size of the aqueous reverse micellar core.[11] Vinogradov and coworkers found noted differences in fluorescence decay times between cyanines in bulk solvents and reverse micellar systems.[33] Thus, differences in dye behaviors can be attributed to the fact that these structures can potential induce spatial and orientation limits on molecular processes and fluorescence probes can be used to study these limits by examining their behaviors within them.[11] The effects of incorporating cyanines into these systems also proposes an interest to examine other molecules such as proteins, inside of them as well.

3.1.3 Human serum albumin

Human serum albumin (HSA) accounts for nearly 60% of the protein found in the human circulatory system.[34] With a molecular mass of 66,439 Da, a structure containing a sequence of 585 amino acids with 17 disulfide bonds, its primary function is serving as the major transport of exogenous and endogenous substances.[26] These interactions occur at specific binding sites on the protein each with their own unique characteristics. Located in subdomain IIA, the warfarin-azapropaozone site specifically binds warfarin and other anticoagulants of similar properties.

Subdomain IIIA consists of the indolebenzodiazeine site that specifically binds diazepam and naproxen.[22] These substances bound include unesterified fatty acids, steroids, bilirubin, salicylate, metabolites, and hormones.[26] It has the added function of binding reversibly to organic compounds, thus making it an ideal drug carrier.[22, 26, 34]

3.1.4 Aim of work

Previous studies have shown that several functionalized heptamethine cyanine dyes containing ester moieties showed cytotoxicity in certain cancer cells with no damage to normal cells (Figure 3.2).[35] It was shown that esters have the ability to penetrate cell membranes easily, thus allowing for greater cellular uptake.[35] The group mentions that these properties have made these compounds very attractive for binding with carrier proteins for in vivo applications.

For the following studies, a model dye similar to those used in the study was selected with the difference of shorter side chain lengths. Dye **YY-1-71 DE** contains two esterfied side chains with a heptamethine linker rigidized with a chlorine substituted cyclohexene ring.

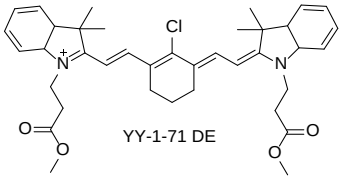

Figure 3.2 Structure of novel heptamethine dye

The versatility of reverse micellar systems makes them ideal models for biological membranes. Specifically, reverse micelles have the added flexibility of providing a confined aqueous core that can vary in size depending on the concentration of water in the system. Thus it is of interest to examine the behavior of these dyes with HSA in the model biomembrane system.

3.1.5 Expected results and hypotheses

It is proposed that utilizing the aqueous core of the reverse micelles for examining the binding interactions between novel dyes and HSA in a more confined environment will increase the binding affinity of the dyes for the protein when compared to binding in the absence of reverse micelles. It is further hypothesized that only protein-bound dye will remain in the aqueous pseudo-phase while, the ester-functionalized free dye will remain either at the surfactant-water pool interface within the reverse micelle.

3.2 Experimental

3.2.1 Instrumentation and software

All absorbance measurements were performed using a Cary UV/VIS/NIR (Lambda 50) Double Beam Spectrophotometer (Norwalk, CT) performed in 1.0 cm quartz cuvettes (Starna Cells, Atascader, CA). All fluorescence measurements were performed in 1.0 cm cuvettes using an ISS K2 spectrofluorometer and all samples were excited using a LaserMaxx laser (Rochester, NY) at appropriate wavelengths. All analyses and linear regressions were performed using Microsoft Excel 2007.

3.2.2 Materials and methods

3.2.2.1 Molar absorptivity determinations

To obtain quantitative data regarding the heptamethine dyes and their interactions with HSA, the molar absorptivity of the dye was determined in PBS and similar measurements were made in the reverse micellar system for comparison. Methods of determination were performed as described in the previous chapter.

3.2.2.2 Dye stock solution preparation

Standard dye indocyanine-green (ICG) was provided by Kodak (Rochester, NY) and the heptamethine cyanine dye **YY-1-71 DE** (**71DE**) was generously provided by the lab of Dr. Maged M. Henary (Georgia State University) , synthesized by Dr. Yogesh Yadav. Stock solutions of each dye were prepared to 1.0 mM by weighing an appropriate mass of each dye directly into 8 mL amber vials to avoid photodegredation. Each dye was dissolved in 200 proof EtOH provided by Koptec (King of Prussia, PA). Experimental concentrations of dye were determined based on limitations set by the spectroscopic instruments.

3.2.2.3 HSA stock solution preparation

Stock solutions of HSA (provided by, Sigma-Aldrich, St. Louis, MO) were prepared to 1.0 mM by dissolving an appropriate mass of solid serum albumin in saline-free PBS (pH 7.4) in appropriate capacity volumetric flasks. Any working stock solutions for the binding studies were prepared from the stock solutions by adding an appropriate volume of stock to a 5 mL volumetric flask, and diluting the sample by filling the flask with pH 7.4 PBS up to the mark. Fresh protein solutions were prepared as necessary for each experiment.

3.2.2.4 Ternary system solution preparation

The surfactant sodium dioctyl sulfosuccinate (AOT) was provided by Sigma-Aldrich (St. Louis, MO) and was used without further purification. An appropriate mass of surfactant was weighed on an analytical balance and was dissolved in n-heptane (J.T. Baker, Center Valley, PA) to a final concentration of 0.10 M.

3.2.2.5 Determination of water pool size

When studying such species in reverse micellar systems, the size of the water pool can be varied based on the amount of water added to the surfactant system. For studies pertaining to bioanalytical applications, it was desired to utilize a water pool that corresponds to a biological compartment or cellular component.

Furthermore, when studying these systems with a protein, the water pool must be of a size necessary to accommodate it. According to Zhang and coworkers, a study of bergenin and HSA in reverse micelles showed that an ideal water pool size for accommodating the protein was found to be 16. They refer to a study conducted by Andrade and coworkers who mention that the ratio of the size of the empty micelle and that of the protein is a crucial factor for protein incorporation; specifically regarding enzyme catalysis. For the nature of the work involving dye and protein binding, it is desirable for the protein in question to maintain its functionality without disturbing its active sites.

Andrade states that the general consensus regarding the ideal water pool size for an enzyme to maintain its functionality is when the radius of sphericity of the protein (r_p) equals the radius of the inner core of the micelle, (r_m). The value of r_p and r_m are found according to:

$$r_p = 0.7x(Mr)^{1/3}$$

$$r_m = 1.5W+4.0$$

with both final values in angstroms, where Mr is the molecular weight of the protein and W is the value of the water pool. Given that these experiments are utilizing HSA, the value of r_p was determined to be 28.4 angstroms or 2.84 nm. Thus a water pool in the AOT reverse micellar

system would have to be large enough to accommodate at least one molecule of protein. Given a series of water pool values 2 – 50, calculate r_m values ranged from 0.44 to 7.6 nm. A water pool value of 20 gives a calculated r_m value of 3.1 nm. Furthermore, according to Nikolenko and coworkers, the size of the hydrodynamic radius of the AOT/alkane system, can be determined by the following expression:

$$R_H = 0.175W + 1.5$$

where R_H is the hydrodynamic radius in nanometers and W is the concentration of water in the system divided by the concentration of AOT in the system ($W=[H_2O]/[AOT]$). Furthermore, they mention that the thickness of the AOT layer at the water/surfactant interface is 0.9 nm and the diameter of the water pool in this system is given by: $d = 0.35W + 1.2$ or $(R_H – 0.9) \times 2$. Thus it can be observed that d is proportional to W, wherby increasing the concentration of water in the system is ultimately increasing the size of the water pool.

3.2.2.6 Calculation of protein accommodation in desired water pool

Protein accommodation was estimated by assuming sphericity of the protein and the water pool. Thus the volumes of the water pool and protein were calculated to be 165 nm^3 and 92 nm^3 respectively. These determinations show that theoretically only one protein can be accommodated by a water pool this size. Additionally, a theoretical number of water pools was calculated by using hard sphere approximations for the size of the water pool with respect to the volumes of individual water molecules. In this regard, the concentration of water in each sample was fixed at 2 M for a water pool size of W=20. It was determined that one water pool could theoretically hold 5E+04 molecules of water and thus 5E+15 total water pools were calculated for each sample which was taken to be the number of reverse micelles in each sample.

It should be mentioned that the values obtained above were determined for sample preparations and theoretical considerations. As mentioned previously, reverse micellar systems are highly dynamic and thus specificity regarding exact size and shape cannot be determined solely by calculations. This dynamic behavior will also be taken into account in the analysis of the obtained results. Furthermore, it should also be mentioned that above specific water pool sizes, terminology shifts from “reverse micelle” to “reverse microemulsion.” Given that spectrally the formation of pure reverse micelles or microemulsions cannot be determined via the spectroscopic techniques in this study, the surfactant system described will be referred to from here on out as the “ternary system”. This system is one made up of AOT, *n*-heptane, and water.

3.2.2.7 Cyanine dye incorporation into the ternary system

Methods of dye incorporation were based off of techniques found in literature by McPhee and coworkers, Nikolenko and coworkers, Sahoo and coworkers, and Zhang and coworkers.[11, 30-31, 36]. Water-insoluble dye incorporation was done by placing an appropriate amount of dye stock solution in an adaptable vial and the solvent was evaporated under a high pressure vacuum. Appropriate portions of PBS at pH 7.4 were added to the dry dye, to which 5.5 mL of 0.10 M AOT/n-heptane stock was added. Water soluble dyes were prepared directly in PBS at pH 7.4 to which that AOT/n-heptane solution was added. The solutions were vortexed to mix. Some mixtures turned turbid, upon which they were left to sit until optically clear solutions were obtained. In early experiments, turbid samples were sonicated for approximately 2 minutes, but this process was terminated to avoid potential damage to the protein.

3.2.2.8 Dye-protein incorporation into the ternary system

Similar procedures were followed for incorporating dye and protein solutions into the ternary system. To the dry dye, an appropriate amount of protein solution dissolved in PBS was

added to the dry dye and the remaining amount of PBS was added to obtain the desired water pool size. Water soluble dyes prepared in PBS were combined with protein solutions and additional PBS as needed. Appropriate amounts of AOT/heptane stocks were then added to these solutions and vortexed to mix upon which optically clear solutions were obtained.

3.2.2.9 Binding studies with protein and cyanine dye

The Scatchard method was employed for determining the binding interactions between the dye and HSA wherein increasing micromolar concentrations of HSA were added to a constant concentration of dye.

3.3 Results and Discussion

3.3.1 Diesterfied dye interactions with HSA outside and within the ternary system

3.3.1.1 Cyanine dye binding with HSA in bulk phosphate buffer

A spectroscopic binding study was conducted with **71DE** and HSA in bulk phosphate buffer. It can be observed that the addition of increasing micromolar concentrations of HSA leads to a concomitant increase in absorbance. Additionally, the dye experiences a gradual red shift of 10 nm as more protein is added before finally leveling out around 10 μM. It can be inferred that the unbound form of the dye is present at 773 nm while the bound form has a λ_{max} at 783 nm.

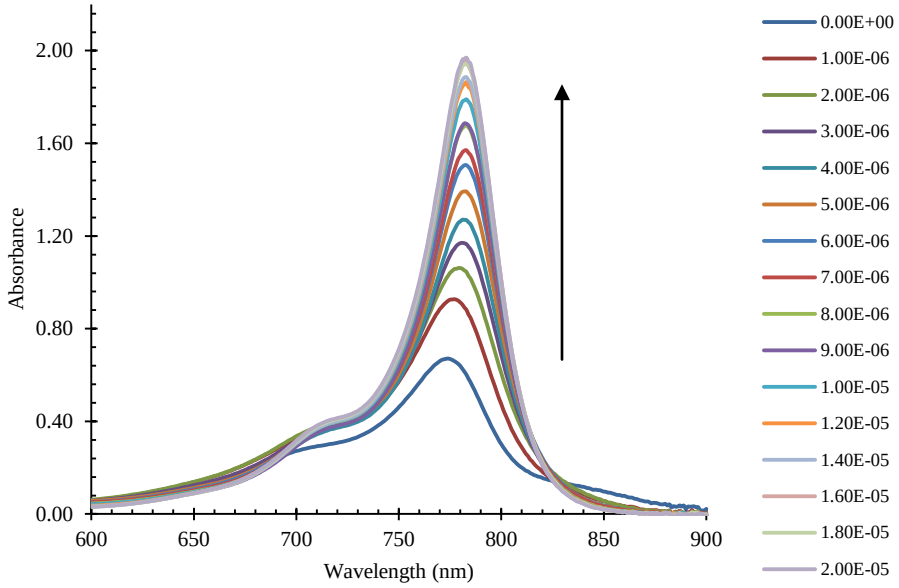

Figure 3.3 71DE with increasing HSA concentration from 0 – 20 µM in bulk PBS

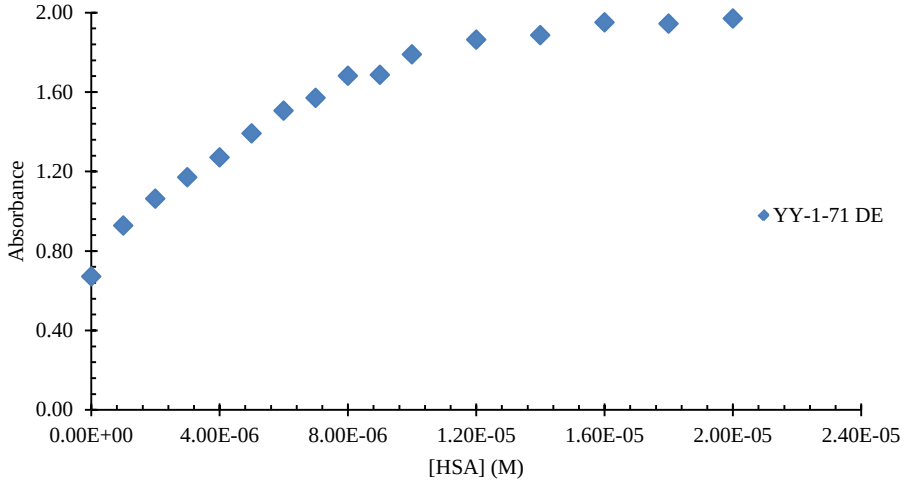

Figure 3.4 Absorbance as a function of HSA concentration of 71DE in bulk PBS

The gradual changes in the dye spectra suggest that no major changes are occurring with the state of the dye other than the presence of the protein. It can be observed that there was some slight aggregation of the dye observed before protein was added; however, the dye remained mostly in its monomeric form as protein concentration increased.

3.3.1.2 Molar absorptivity determination

The molar absorptivity of the free dye was also determined in bulk PBS. As expected, the dye behaved in accordance with Beer's Law as there was a linear increase in absorbance as the concentration of dye was increased. It was found that **71DE** has a molar absorptivity value of 1.7E+05 $M^{-1}cm^{-1}$ at 773 nm (Figures 3.5 and 3.6).

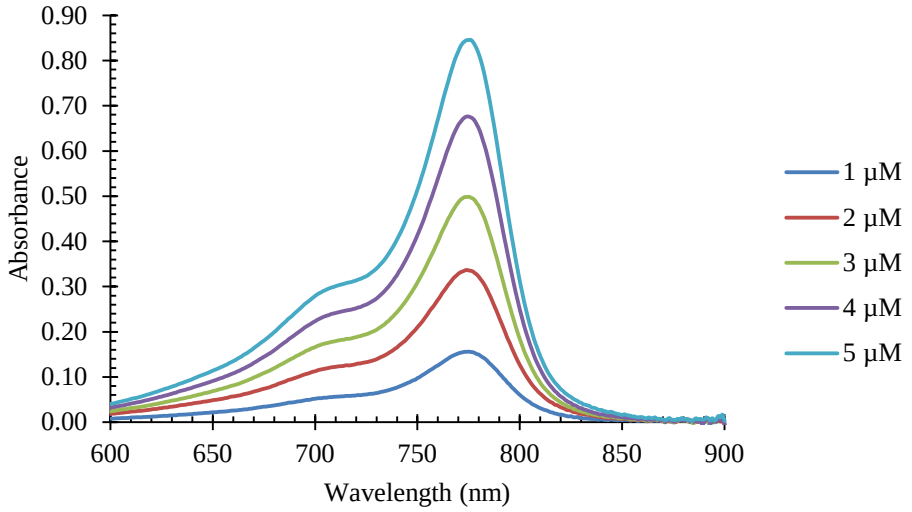

Figure 3.5 Absorbance as a function of wavelength of 71DE in bulk PBS

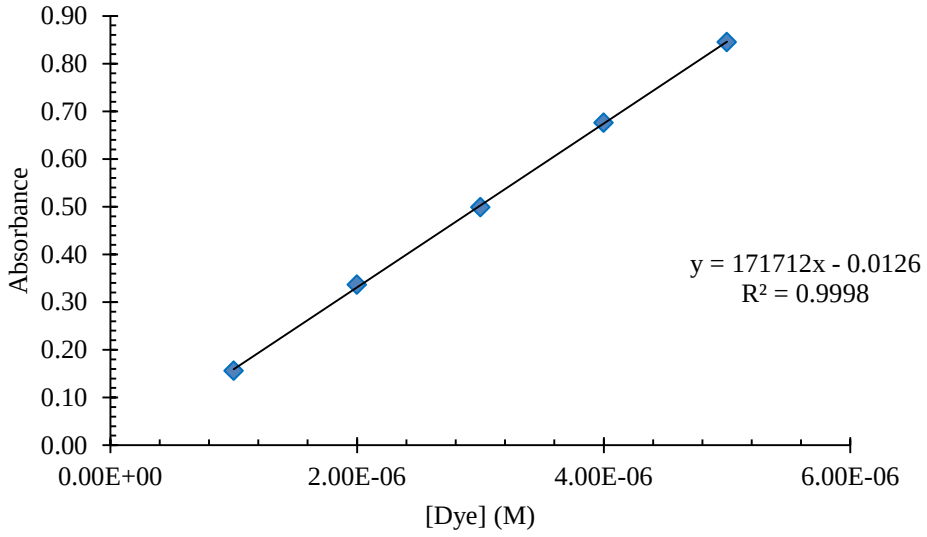

Figure 3.6 Absorbance as a function of 71DE concentration in bulk PBS

As mentioned previously by Kim, more accurate binding constants can be obtained when the absorbance peak of the bound and free forms of dye are markedly different. While there was a noticeable redshift in absorbance, binding data was obtained via fluorescence measurements for assurance.

3.3.1.3 Fluorescence studies

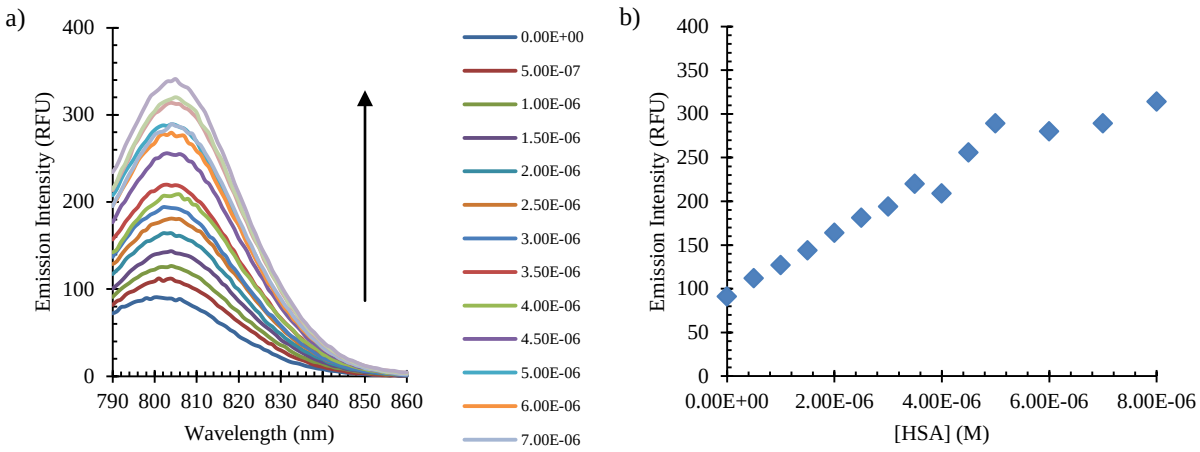

Figure 3.7 a) Emission of 71DE as a function of wavelength b) Emission intensity of 71DE as a function of HSA concentration from 0 – 10 µM

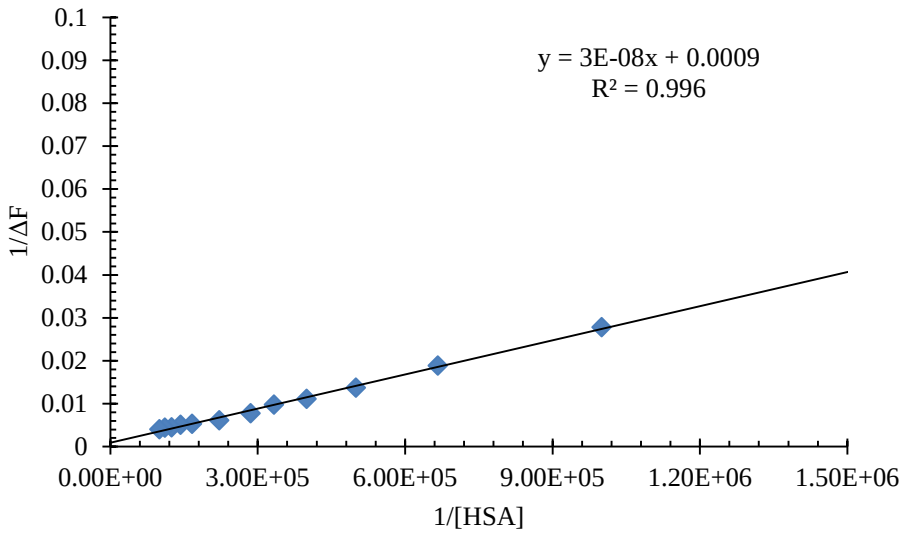

Figure 3.8 Modified Scatchard Plot of 71DE and HSA binding interactions

The Scatchard method was employed for determining the binding interactions between the diesterfied dye and HSA. There was a marked increase in fluorescence intensity as well as a redshift in wavelength. The double reciprocal plot yielded a straight line thus corresponding to the binding activities of the two species (Figure 3.8). The binding constant of the dye was calculated by obtaining the equation of the line and dividing the intercept by the slope. The obtained K value was found to be 7.1E+04 with a Free Energy (ΔG) of -2.5E+04 J/mol.

The above experiments show how the dye interacts with HSA under bulk solvent conditions with consistent trends and binding data could be obtained.

3.3.2 Diesterfied dyes binding with HSA in the ternary system

3.3.2.1 Determination of molar absorptivity in the ternary system

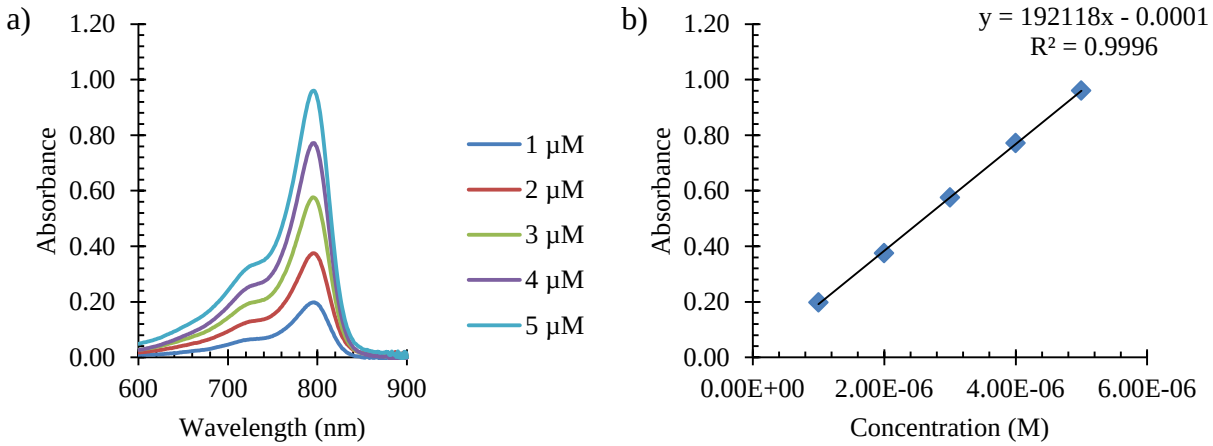

Figure 3.9 a) Absorbance as a function of wavelength of YY-1-71 DE from 0 – 5 µM in the ternary system b) Absorbance as a function of dye concentration in the ternary system

The molar absorptivity of **YY-1-71 DE** was obtained in ternary system without the addition of protein (Figure 3.9). The dye experienced a 23 nm red shift when in the reverse micellar system with a λ_{max} at 796 nm. It was found that the molar absorptivity was only slightly higher in ternary system than in bulk PBS with a value of 1.9E+05 $M^{-1}cm^{-1}$. Figure 3.10 shows a comparison of the dye's spectral shape in bulk PBS compared to that of confined PBS. There is a noticeable increase in monomerization when the dye is in the ternary system as indicated by the sharpened and larger absorption band at 796 nm.

This monomerization is not unusual for the dye in such as system; as stated previously, micelles and reverse micelles are known for their solubilization properties. Assuming that in the ternary system, reverse micelles or microemulsions do form, the aggregation behavior would be minimized due to its solubilization.

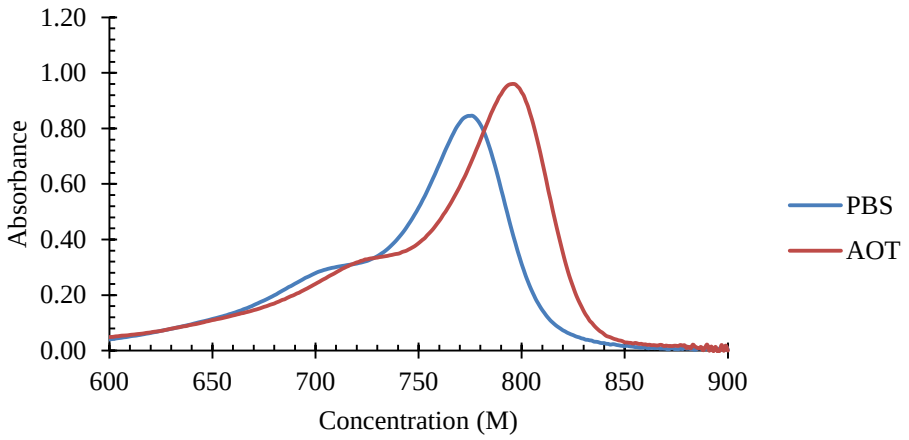

Figure 3.10 Absorbance spectra of 5 µM 71DE in bulk PBS compared to confined PBS in the AOT ternary system

Given that the dye is prevented from additional aggregation, this observation could also give clues as to where the dye could possibly be located within the in system. The dye itself is insoluble in PBS and *n*-heptane; however it is positively charged as opposed to the negatively charged surfactant head groups. The prevented aggregation could suggest that the dye is residing within the pseudo-phase of the surfactant and the water pool. This pseudo-phase is one described as the apparent interface between the surfactant head groups and the water molecules if indeed true microemulsions formed.

The results obtained are similar to those obtained by Vinogradov and coworkers who attribute the interfacial residence to electrostatic interactions between the oppositely charged dye and surfactant.[33] Based on interactions between the oppositely charged dye and surfactant, it was then of interest to see if these interactions would be compromised or changed with the addition of HSA.

3.3.3 Cyanine dye interactions with HSA in the ternary system

A series of experiments were conducted to examine the effects of dye concentration as well as protein concentration in the ternary system to investigate any apparent changes between the dye-protein interactions.

As mentioned previously, theoretical calculations suggested that if they were to form, one reverse micelle with a water pool size of 20 can accommodate one molecule of protein. Figures 3.11a and b show the effects of protein concentration on 5 µM of dye with increasing concentration of HSA in the ternary system.

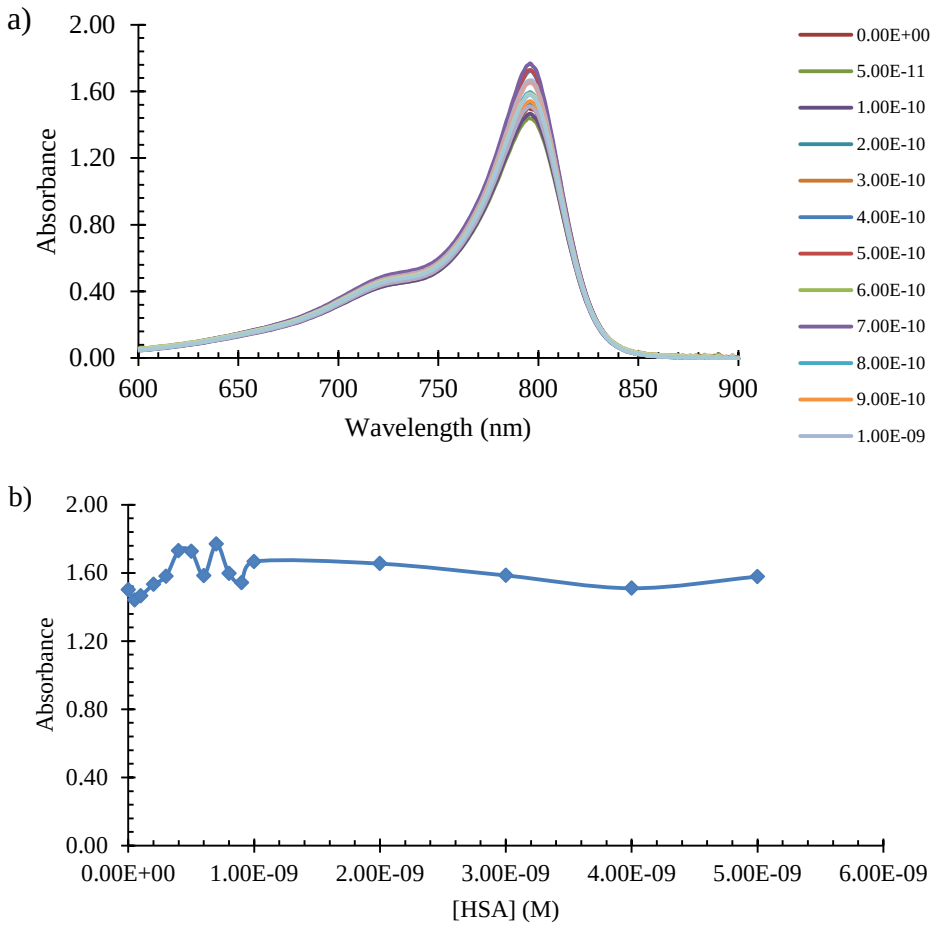

Figure 3.11 Absorbance as a function of 5 µM YY-1-71 DE a) Wavelength with increasing [HSA] from 0 – 5.0 nM in the ternary system b) 71DE as a function of increasing [HSA]

Under these conditions, it was calculated that the theoretical number of protein molecules encapsulated ranged from 0 – 8E+14 out of a system of 5E+15 theoretical reverse micelle water pools, which leaves 17% of potential water pools unoccupied. The maximum absorbance wavelength of the dye remained unchanged at 796 nm throughout the experiment even after addition of the protein. This suggests that the dye remains in a similar environment (i.e. at the pseudo-phase) and minor fluctuations could be attributed to disturbances from the protein molecules occupying the water pools. Furthermore, it is apparent that even the addition of protein does not compromise the electrostatic effects of the dye and the surfactant head group.

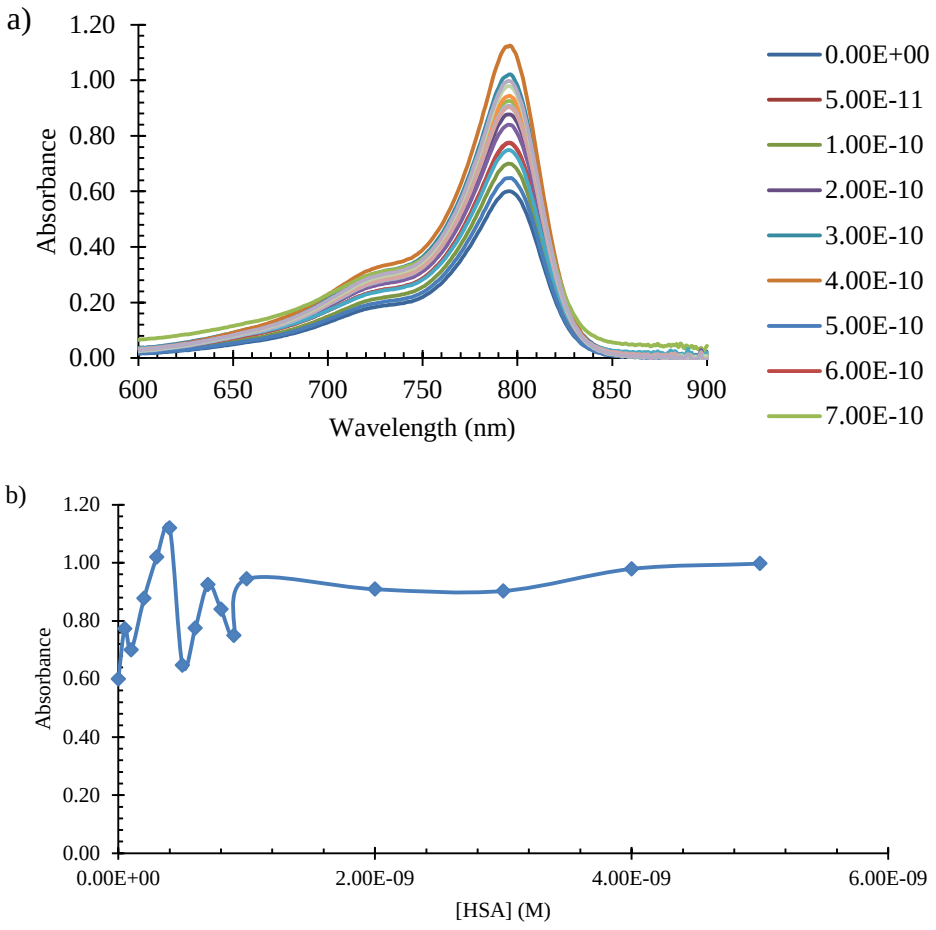

Figure 3.12 a) Absorbance as a function of wavelength of 2.5 µM YY-1-71 DE with [HSA] from 0 – 5.0E-9M b) 71DE Absorbance as a function of [HSA] concentration in the ternary system

Figure 3.12 shows that lowering the concentration of the dye amplified the slight changes in absorbance by displaying an increase in dye absorbance as the concentration of protein was increased from 0 – 0.4 nM before decreasing again, then leveling out around 1 nM as in the previous experiment.

In bulk PBS wherein the movement of the protein is not restricted and other molecules are free to interact with one another, the dye and protein show signs of binding interactions in. However, in the ternary system, given solubility constraints of the protein, it is suggested that HSA would remain in the aqueous core while the dye appears to have no interactions with the protein.

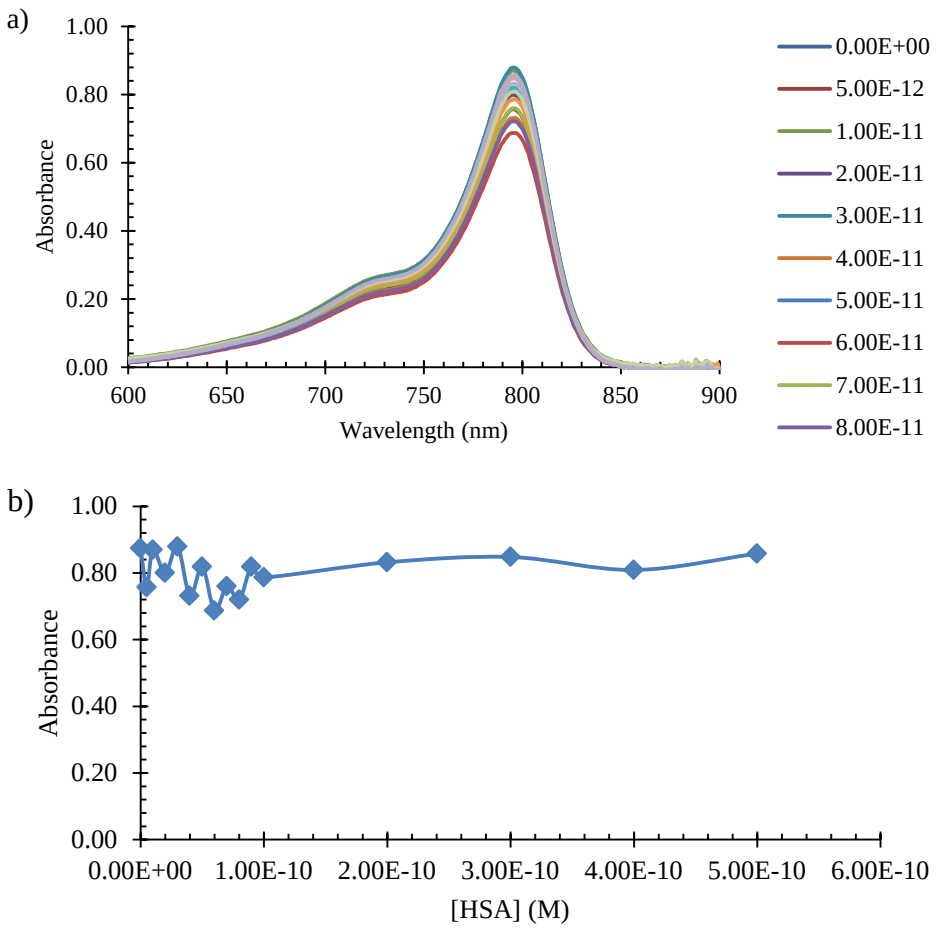

Figure 3.13 Absorbance as a function of wavelength of 2.5 µM YY-1-71 DE with [HSA]= 0 – 0.5 nM

Given that theoretically, only a portion of the water pools were occupied by protein, it is more likely that dye residing the pseudo-phase of the ternary system wherein a water pool not occupied by protein would experience less perturbation.

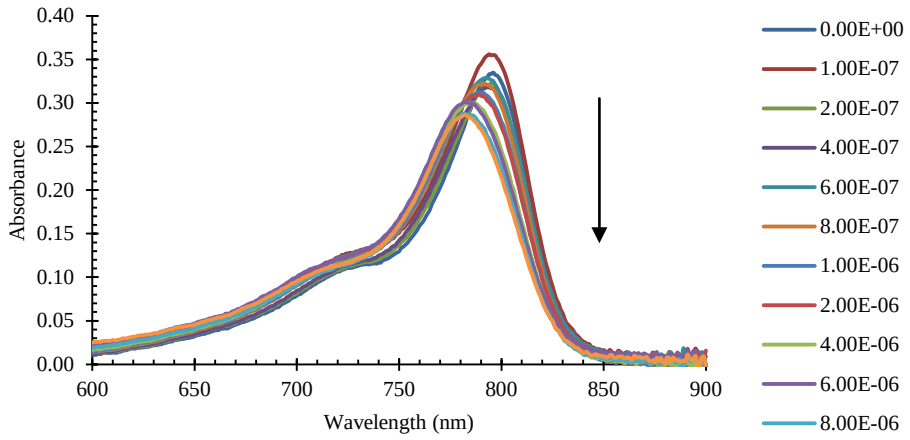

Figure 3.14 Absorbance as a function of wavelength of 1 µM YY-1-71 DE with increasing [HSA] from 0 - 10µM in the ternary system

Figure 3.15 shows the absorbance spectra when the concentration of dye was lowered to 1 µM and the concentration of protein was increased from 0 – 10 µM. The results of this experiment showed that an over saturation of the theoretical water pools causes the dye experiences a blue shift in absorbance from 795 to 784 nm, wherein 784 nm is around the same wavelength as the bound dye in bulk PBS. Furthermore, the absorbance spectra show a decrease in absorbance of the monomer band as the concentration of protein increased (Figure 3.16).

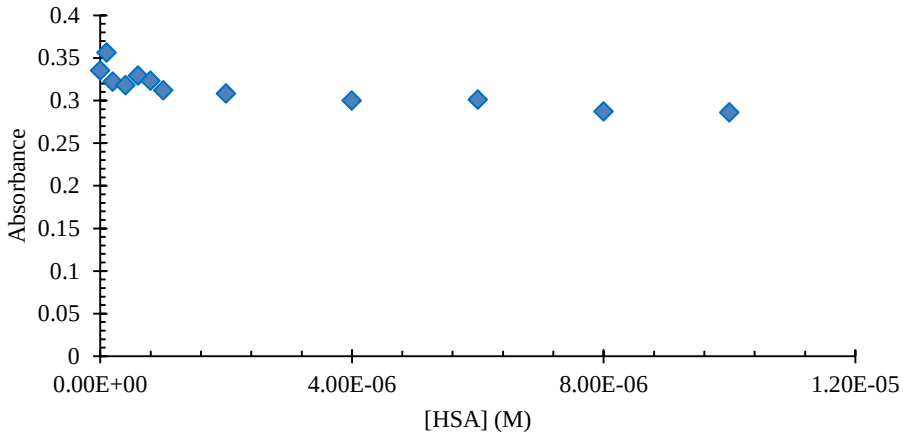

Figure 3.15 1μM 71DE absorbance as a function of [HSA] from 0 – 10 μM in the ternary system

Under these conditions, theoretically, the number of protein molecules exceeded that of the available number of water pools. It is clear that the protein would experience denaturation in the hydrophobic organic solvent, thus keeping suggesting that is remain in the water pool if such microemulsions were formed. Therefore, it can be hypothesized that there was a shift in the equilibrium of the system that allowed the water pools to somehow rearrange themselves to accommodate the rest of the proteins or some of the protein was denatured. No turbidity was observed in these samples which is generally a sign of an unstable system and typically W values above 30 tend to decrease in stability.[30]

3.3.4 Fluorescence studies in the ternary system

To gain more insight regarding the cyanine dye localization and behavior, a study of the dye's fluorescence under these conditions was conducted.

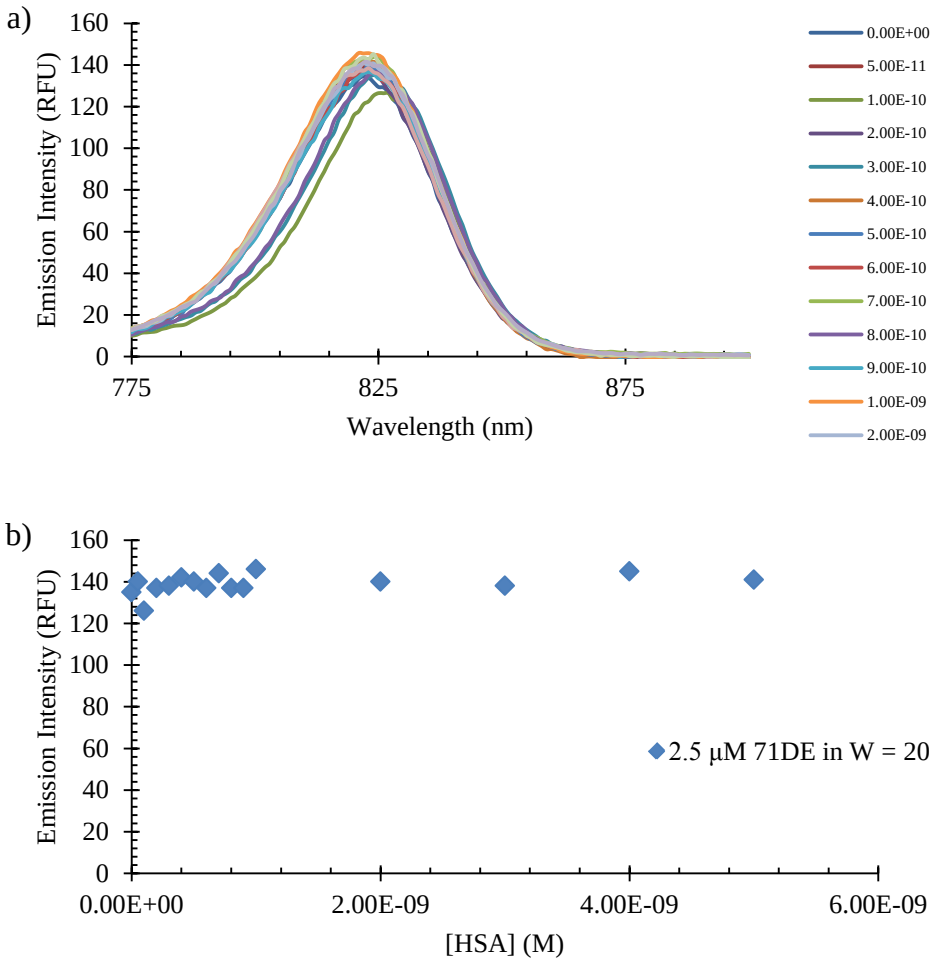

Figure 3.16 Emission of 71DE a) as a function of wavelength b) a function of HSA concentration in the ternary system

The fluorescence spectra of **71DE** in the ternary system show very different behavior in when compared to the bulk PBS system. Figure 3.16 shows that there was no increase in emission intensity of the dye as the concentration of protein was increased.

In the ternary system, there was an observed red shift which fluctuated between 822 and 826 nm; whereas in bulk PBS, the Em_{max} was found to increase from 800 – 805 nm. These results further confirm that the dye behaves differently in bulk solvents when compared to the ternary system. However, given the theoretical assumptions, it should be noted that these differences cannot be contributed solely to confinement. As the absorbance and emission spectra

gave no clear dependency on protein concentration as those observed in bulk PBS, it is strongly suggested that the dye is associating with the oppositely charged surfactant head group.

3.3.5 Effects of dye concentration on spectral behavior in the ternary system

While the results show that the protein concentration has little effect on the apparent behavior of the dye, it was of interest to see how the spectra of the dye changed when theoretically all of the water pools in the ternary system were occupied. Due to the instrumental limitations of absorbance spectrometers, a fluorescence study was carried out to see if the dye concentration had an effect on the spectral behavior in the ternary system. Theoretical calculations determined that 1.2E-08 M of HSA would be enough protein to occupy all of the calculated water pools if such a system existed in the samples prepared. The results are shown in Figure 3.17.

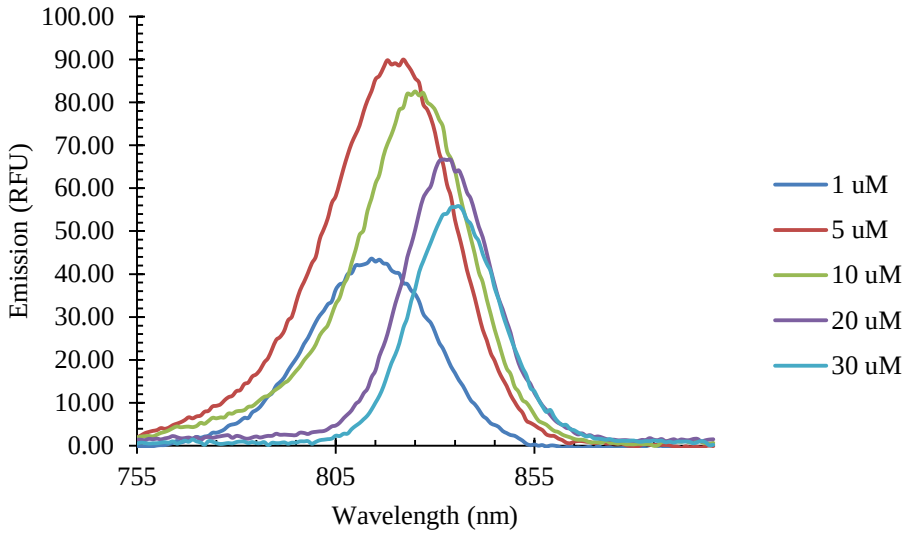

Figure 3.17 Emission as a function of wavelength of increasing concentrations of **71DE** in the ternary system with 1.2E-08 M HSA.

It can be observed in the ternary system that when the concentration of protein remained constant with all of the theoretical number of water pools occupied, increasing the dye

concentration led to an initial increase in fluorescence intensity before experiencing a subsequent red shift in the emission spectra. The red shift observed was from 814 nm to 836 nm at the various concentrations. Comparing this data to that obtained above, it was found that through fluorescence studies before all of the theoretical water pools were occupied, in the ternary system, **71DE** has an emission wavelength of 822 nm and 826 nm.

At 5 μM dye, in the ternary system with all of the theoretical water pools occupied, the dye also has an emission wavelength of 822 nm. This result suggests that at 5 μM, the dye is still associating with the surfactant headgroups. As the concentration of dye increased, the emission wavelength shifted to lower energies up to 836 nm at 30 μM of dye. Given that the precise formation of reverse micelles or microemulsions cannot be confirmed from this data changes in localization of the dye cannot be confirmed. However, based on what is known, decreases in fluorescence intensity as a result of a high concentration of dye can lead to the inner filter effect as described in the previous chapter. Thus, it could be that the dye is experiencing some type of self-quenching due to the increase of dye monomers in the system.

Moreover, as mentioned previously, true reverse micelles are not spherical in shape and varying the concentration of water in the system further distorts the shape of the micelle. The above results could suggest that if reverse micelles or microemulsions did form, the addition of copious amounts of dye with all water pools occupied by protein caused such a distortion in the ordered system that the system became unstable and was thus destroyed. Therefore, it can further be suggested that incorporating cyanines in to the ternary system could theoretically alter the equilibrium of formation of these ordered structures.

3.4 Conclusions

A study was conducted to observe the binding interactions between functionalized heptamethine cyanine dyes and HSA in bulk and biomembrane mimetic solvent systems. The results of the studies showed that the dye interactions with the protein in the bulk solvent system varied greatly from those observed in ternary AOT/*n*-heptane/water system. Dye **YY-1-71 DE** showed consistent behavior in binding with HSA in bulk PBS with a gradual increase in absorbance and red shift in wavelength. However, when introduced with the protein into the ternary system, there was no such change. Instead, it can be suggested that due to the electrostatic interactions between the oppositely charge dye and surfactant head group that the dye remains at the theoretical pseudo-phase of the water pool and surfactant head group if reverse micelles or microemulsions did form. Adjustments with dye and protein concentrations show that the lowering the concentration of protein lessens the disturbance of the dye's polymethine chain while in the ternary system thus leading to subtle changes of the absorbance spectra. Moreover, additional studies would be needed to determine the true location of the dye molecules in the ternary system.

The emission behavior of the system differs in bulk PBS from the ternary system's conditions as well. Spectral behaviors consistent with that of the dye's location in the pseudo-phase are evident by the lack of change in the emission intensity as well as the emission wavelength. Furthermore, when all of the theoretical water pools were occupied by protein, increasing the concentration of the dye in the system caused a decrease in emission intensity as well as a red shift in the emission wavelength. This was thought to be the result of the inner filter effect or perhaps the severe distortion of the proposed reverse micellar system.

The formation of true reverse micelles and microemulsions would need to be confirmed via techniques beyond the capabilities of the instrumentation used in these studies. However, they were suitable for investigating dye and protein binding in bulk solvent systems. Furthermore, these studies provided starting points for investigating dye interactions with protein in more complex systems such as those that could be possibly encountered *in vivo.*

REFERENCES

1. Hamer, F. M., *The cyanine dyes and related compounds*. Interscience Publishers: London, 1964.

2. Venkataraman, K., *Synthetic Dyes*. Academic Press: London, 1952; Vol. 1.

3. Venkataraman, K., *Synthetic Dyes*. Academic Press: London, 1952; Vol. 2.

4. Peters, A. T., Freeman, H.S., *Analytical chemistry of synthetic colorants*. Blackie Academic & Professional: London, 1995; Vol. 2.

5. Sun, S.; Chen, P.; Zhou, S.; Qian, Z.; Zheng, D.; Tsuneki, O.; Masaaki, H., Optical and thermal properties of a cyanine dye medium for next-generation DVD-Rs. *Imaging Sci. J.* **1999,** *47* (2), 113-117.

6. Tani, T.; Seki, K.; Yoshihara, K.; Hanna, J., Thin organic layers for photography and electronic devices. *Int. J. Photoenergy* **2006,** (5), 2/1-2/8.

7. Engel, T., *Quantum Chemistry and Spectroscopy*. 3rd ed.; Pearson Education, Inc.: Glenview, 2013.

8. Harris, D. C., *Quantitative Chemical Analysis*. Eighth ed.; W.H. Freeman and Company: New York, 2010.

9. Kuhn, H., A Quantum Mechanical Theory of Light Absorption of Organic Dyes and Similar Compounds. *The Journal of Chemical Physics* **1949,** *17* (12), 1198-1212.

10. Peters, A. T., Freeman, H.S., *Colour Chemistry*. Elsevier Science Publishing Company: New York, 1991.

11. Nikolenko, L. M.; Ivanchihina, A. V.; Brichkin, S. B.; Razumov, V. F., Ternary AOT/water/hexane systems as "micellar sieves" for cyanine dye J-aggregates. *J. Colloid Interface Sci.* **2009,** *332* (2), 366-372.

12. Beckford, G.; Owens, E.; Henary, M.; Patonay, G., The solvatochromic effects of side chain substitution on the binding interaction of novel tricarbocyanine dyes with human serum albumin. *Talanta* **2012,** *92*, 45-52.

13. Guralchuk, G. Y.; Katrunov, I. K.; Grynyov, R. S.; Sorokin, A. V.; Yefimova, S. L.; Borovoy, I. A.; Malyukin, Y. V., Anomalous surfactant-induced enhancement of luminescence quantum yield of cyanine dye J-aggregates. *J. Phys. Chem. C* **2008,** *112* (38), 14762-14768.

14. Drobizhev, M.; Sigel, C.; Rebane, A., Picosecond fluorescence decay and exciton dynamics in a new far-red molecular J-aggregate system. *J. Lumin.* **2000,** *86* (2), 107-116.

15. Behera, G. B.; Behera, P. K.; Mishra, B. K., Cyanine dyes: self aggregation and behavior in surfactants a review. *J. Surf. Sci. Technol.* **2007,** *23* (1-2), 1-31.

16. Kim, J. S.; Kodagahally, R.; Strekowski, L.; Patonay, G., A study of intramolecular H-complexes of novel bis(heptamethine cyanine) dyes. *Talanta* **2005,** *67* (5), 947-54.

17. Sun, H.; Xiang, J.; Zhang, X.; Chen, H.; Yang, Q.; Li, Q.; Guan, A.; Shang, Q.; Tang, Y.; Xu, G., A colorimetric and fluorometric dual-modal supramolecular chemosensor and its application for HSA detection. *Analyst (Cambridge, U. K.)* **2014,** *139* (3), 581-584.

18. Guo, Z.; Nam, S.; Park, S.; Yoon, J., A highly selective ratiometric near-infrared fluorescent cyanine sensor for cysteine with remarkable shift and its application in bioimaging. *Chem. Sci.* **2012,** *3* (9), 2760-2765.

19. Shimizu, Y.; Temma, T.; Hara, I.; Yamahara, R.; Ozeki, E.-i.; Ono, M.; Saji, H., Development of novel nanocarrier-based near-infrared optical probes for in vivo tumor imaging. *J. Fluoresc.* **2012,** *22* (2), 719-727.

20. Williams, R. J.; Lipowska, M.; Patonay, G.; Strekowski, L., Comparison of covalent and noncovalent labeling with near-infrared dyes for the high-performance liquid chromatographic determination of human serum albumin. *Anal Chem* **1993,** *65* (5), 601-5.

21. Sun, C.; Zhou, S.; Chen, P., Influences of Na+ and H+ on the spectroscopic properties and morphologies of a cyanine dye. *Dyes Pigm.* **2005,** *67* (3), 211-214.

22. Kim, H. S.; Austin, J.; Hage, D. S., Identification of drug-binding sites on human serum albumin using affinity capillary electrophoresis and chemically modified proteins as buffer additives. *Electrophoresis* **2002,** *23* (6), 956-963.

23. Loughney, J. W.; Lancaster, C.; Ha, S.; Rustandi, R. R., Residual bovine serum albumin (BSA) quantitation in vaccines using automated Capillary Western technology. *Analytical biochemistry* **2014,** *461*, 49-56.

24. Vicente-Serrano, J.; Caballero, M. L.; Rodríguez-Pérez, R.; Carretero, P.; Pérez, R.; Blanco, J. G.; Juste, S.; Moneo, I., Sensitization to serum albumins in children allergic to cow's milk and epithelia. *Pediatric Allergy and Immunology* **2007,** *18* (6), 503-507.

25. Pisoni, D. S.; Todeschini, L.; Borges, A. C. A.; Petzhold, C. L.; Rodembusch, F. S.; Campo, L. F., Symmetrical and Asymmetrical Cyanine Dyes. Synthesis, Spectral Properties, and BSA Association Study. *J. Org. Chem.* **2014,** *79* (12), 5511-5520.

26. Anraku, M.; Yamasaki, K.; Maruyama, T.; Kragh-Hansen, U.; Otagiri, M., Effect of oxidative stress on the structure and function of human serum albumin. *Pharm. Res.* **2001,** *18* (5), 632-639.

27. Yvon, J. A Guide to Recording Fluorescence Quantum Yields. http://www.horiba.com/fileadmin/uploads/Scientific/Documents/Fluorescence/quantumyieldstrad.pdf.

28. Tatikolov, A. S.; Costa, S. M. B., Complexation of polymethine dyes with human serum albumin: a spectroscopic study. *Biophys Chem* **2004,** *107* (1), 33-49.

29. Levitz, A.; Ladani, S. T.; Hamelberg, D.; Henary, M., Synthesis and effect of heterocycle modification on the spectroscopic properties of a series of unsymmetrical trimethine cyanine dyes. *Dyes Pigm.* **2014,** *105*, 238-249.

30. Zhang, Y.; Dong, L.; Li, Y.; Li, J.; Chen, X., Characterization of Interaction Between Bergenin and Human Serum Albumin in Membrane Mimetic Environments. *J. Fluoresc.* **2008,** *18* (3-4), 661-670.

31. Sahoo, D.; Bhattacharya, P.; Chakravorti, S., Reverse Micelle Induced Flipping of Binding Site and Efficiency of Albumin Protein with an Ionic Styryl Dye. *J. Phys. Chem. B* **2010,** *114* (32), 10442-10450.

32. Luisi, P. L., Straub, B.E., *Reverse Micelles*. Plenum Press: New York, 1982.

33. Vinogradov, A. M.; Tatikolov, A. S.; Costa, S. M. B., The effect of anionic, cationic and neutral surfactants on the photophysics and isomerization of 3,3'-diethylthiacarbocyanine. *Phys. Chem. Chem. Phys.* **2001,** *3* (19), 4325-4332.

34. Zhu, J.; Wu, L.; Zhang, Q.; Chen, X.; Liu, X., Investigation of the interaction of Daphnin with human serum albumin using optical spectroscopy and molecular modeling methods. *Spectrochim. Acta, Part A* **2012,** *95*, 252-257.

35. Henary, M.; Pannu, V.; Owens, E. A.; Aneja, R., Near infrared active heptacyanine dyes with unique cancer-imaging and cytotoxic properties. *Bioorg. Med. Chem. Lett.* **2012,** *22* (2), 1242-1246.

36. McPhee, J. T.; Scott, E.; Levinger, N. E.; Van Orden, A., Cy3 in AOT Reverse Micelles I. Dimer Formation Revealed through Steady-State and Time-Resolved Spectroscopy. *J. Phys. Chem. B* **2011,** *115* (31), 9576-9584.